CLINICAL REPORT

AMERICAN JOURNAL OF medical genetics PART A

# A de novo 1.4-Mb Deletion at 21q22.11 in a Boy With Developmental Delay

**Ryoko Fukai,[1,2] Yoko Hiraki,[3] Gen Nishimura,[4] Mitsuko Nakashima,[1] Yoshinori Tsurusaki,[1] Hirotomo Saitsu,[1] Naomichi Matsumoto,[1]* and Noriko Miyake[1]***

[1]Department of Human Genetics, Yokohama City University Graduate School of Medicine, Yokohama, Japan

[2]Department of Neurology and Stroke Medicine, Yokohama City University Graduate School of Medicine, Yokohama, Japan

[3]Hiroshima Municipal Center for Child Health and Development, Hiroshima, Japan

[4]Department of Pediatric Imaging, Tokyo Metropolitan Children's Medical Center, Fuchu, Tokyo, Japan

Manuscript Received: 14 September 2012; Manuscript Accepted: 20 October 2013

Monosomy 21 is a very rare chromosomal abnormality. At least 45 patients with partial deletion involving 21q11 have been reported. Here, we report a Japanese boy who presented with pre- and postnatal growth delays, psychomotor developmental delay, microcephaly, and iris coloboma. Cytogenetic analysis revealed a de novo 1.4-Mb deletion at 21q22.11 containing 19 protein-coding RefSeq genes. We compared the clinical phenotypes between the present patient and 16 previously reported patients with a deleted region associated with postnatal growth delay and psychomotor developmental delay. Interestingly, *ITSN1* was the only gene deleted or disrupted in all cases; this gene is known to be associated with intellectual disability. Microcephaly and brain structural abnormalities including polymicrogyria and agenesis/hypoplasia of the corpus callosum may also result from haploinsufficiency of *ITSN1*, highlighting its clinical significance for the neurological features of patients with monosomy 21. © 2014 Wiley Periodicals, Inc.

**Key words:** 21q22.11 deletion; developmental delay; fluorescence in situ hybridization (FISH); copy number analysis; *ITSN1*

How to Cite this Article:
Fukai R, Hiraki Y, Nishimura G, Nakashima M, Tsurusaki Y, Saitsu H, Matsumoto N, Miyake N. 2014. A de novo 1.4-Mb deletion at 21q22.11 in a boy with developmental delay.
Am J Med Genet Part A 9999:1–8.

## INTRODUCTION

Monosomy 21 is a very rare chromosomal abnormality compared with trisomy 21, which is the most common chromosomal abnormality in humans [Albert, 2001]. It is possible that fetuses with full monosomy 21 die before or soon after birth [Courtens et al., 1994; Huret et al., 1995; Oegema et al., 2010]. In contrast, at least 45 patients with partial deletion of chromosome 21 have been reported [Braddock and Carey, 1994; Courtens et al., 1994; Theodoropoulos et al., 1995; Chen et al., 2003; Yao et al., 2006; Hoyer et al., 2007; Beri-Dexheimer et al., 2008; Shinawi et al., 2008; Lyle et al., 2009; Fujita et al., 2010; Katzaki et al., 2010; Lindstrand et al., 2010; Oegema et al., 2010; Byrd et al., 2011; Click et al., 2011; Melis et al., 2011; Roberson et al., 2011; Thevenon et al., 2011; Izumi et al., 2012]. Among 21q22 microdeletion syndromes, Braddock–Carey syndrome with thrombocytopenia multiple anomalies and intellectual disability was first described in 1994 [Braddock and Carey, 1994]. This syndrome is caused by haploinsufficiency of *RUNX1* [Katzaki et al., 2010; Braddock et al., 2011; Thevenon et al., 2011]. The clinical phenotypes of 21q22 deletion vary from normal to severe, depending on the size and position of the deletion [Courtens et al., 1994; Chettouh et al., 1995; Theodoropoulos et al., 1995; Yao et al., 2006; Beri-Dexheimer et al., 2008; Shinawi et al., 2008; Lyle et al., 2009; Fujita et al., 2010; Katzaki et al., 2010; Lindstrand et al., 2010; Melis et al., 2011; Roberson et al., 2011]. Moreover, three regions for partial monosomy 21 have been proposed based on genotype–phenotype correlation studies

Conflict of interest: none.
Grant sponsor: Ministry of Health, Labour and Welfare of Japan; Grant sponsor: The fund for Creation of Innovation Centers for Advanced Interdisciplinary Research Areas Program in the Project for Developing Innovation Systems; Grant sponsor: Strategic Research Program for Brain Sciences; Grant sponsor: Ministry of Education, Culture, Sports, Science and Technology of Japan; Grant sponsor: Japan Society for the Promotion of Science; Grant sponsor: Takeda Science Foundation; Grant sponsor: Yokohama Foundation for Advancement of Medical Science; Grant sponsor: Hayashi Memorial Foundation for Female Natural Scientists.
*Correspondence to:
Noriko Miyake, MD, PhD, Naomichi Matsumoto, MD, PhD, Department of Human Genetics, Yokohama City University Graduate School of Medicine, Fukuura 3-9, Kanazawa-ku, Yokohama 236-0004, Japan.
E-mail: nmiyake@yokohama-cu.ac.jp; naomat@yokohama-cu.ac.jp
Article first published online in Wiley Online Library (wileyonlinelibrary.com): 00 Month 2014
DOI 10.1002/ajmg.a.36377

[Lyle et al., 2009; Roberson et al., 2011]. These are region 1: deletion from the centromere to 32.3 Mb (hg19), region 2: from 32.3 to 37.1 Mb (hg19), and region 3: 37.1 Mb to the telomere (hg19). Region 2 deletion is likely associated with a severe phenotype [Roberson et al., 2011]. Here, we report a Japanese boy with a de novo 1.4-Mb deletion at 21q22.1 within region 2; this may provide insight into the relationship between the deleted region and the clinical manifestations.

## MATERIALS AND METHODS

### Samples

Peripheral blood samples from the patient and his parents were sent to us after their written informed consent was obtained. DNA was extracted using a QuickGene-610L (Fujifilm, Tokyo, Japan) according to the manufacturer's instructions. The parentage was confirmed using nine polymorphic markers (information available on request). This study was approved by the institutional review board of Yokohama City University School of Medicine.

### Copy Number Analysis

Pathogenic gene copy number variations were analyzed using a CytosScan™ HD array (Affymetrix, Santa Clara, CA) and Chromosome Analysis Suite v1.2 software (Affymetrix) according to the manufacturer's instructions. The detection conditions for Chromosome Analysis Suite were as follows: a confidence value of 90%, 20 contiguous probes, and larger than 100 kb for duplications; and a confidence value of 89%, 20 contiguous markers, and larger than 10 kb for deletions.

### Fluorescence In Situ Hybridization (FISH)

Metaphase chromosomes were prepared from peripheral blood lymphocytes from the patient and his parents according to standard protocols. Four RPCI-11 human bacterial artificial chromosome (BAC) clones were used: RP11-70F1 (chr21:34,038,494–34,212,146 bp according to the University of California Santa Cruz (UCSC) genome browser hg19), RP11-484I8 (chr21: 34,874,308–35,042,949 bp) for the deleted region, RP11-626D11 (chr21: 19,060,470–19,225,491 bp), and RP11-345F15 (chr21: 46,769,379–46,984,213 bp) for reference. BAC DNA was labeled with Green-UDP (Abbott Molecular, Des Plaines, IL) or Cy3-11-dUTP using a Vysis Nick Translation kit (Vysis, Downers Grove, IL). The labeled probes were applied to the chromosomes, incubated at 37°C for 16–72 hr and then washed and mounted in antifade solution (Vector Laboratories, Burlingame, CA) containing 4′,6-diamidino-2-phenylindole. Images were taken on an AxioCam MR charge-coupled device camera fitted to an Axioplan2 fluorescence microscope (Carl Zeiss, Oberkochen, Germany).

## RESULTS

The patient was a 19-month-old boy, born at 38 weeks of gestation to healthy, non-consanguineous Japanese parents as the first child after a normal pregnancy. His birth weight was 2,602 g (−0.7 SD), length 48 cm (−0.2 SD), and occipital–frontal circumference (OFC) 31.0 cm (−1.2 SD). At 11 months old, his height was 72.7 cm (−0.76 SD), weight 7,140 g (−2.26 SD), and OFC 43.3 cm (−1.97 SD). At 19 months, his height was 76.5 cm (−1.6 SD), weight 8,270 g (−2.1 SD), and OFC 46.1 cm (−1.1 SD). He was able to control his head at 10 months, roll over at 13 months and sit alone at 25 months. Based on the Enjoji developmental assessment [Enjoji and Yanai, 1961], his developmental age at 19 months was 6 months and his developmental quotient was 32.

At 11 months, dysmorphic facial features were noted including midface hypoplasia, bilateral coloboma of the iris, low-set ears, broad and low nasal bridge, anteverted nares, downturned corners of the mouth and thin upper lip vermilion (Fig. 1A–D) as well as widely spaced nipples, hypoplasia of the fifth toenails, edematous dorsum of hands and foot, cryptorchidism, and hypotonia. At 17 months, he developed generalized clonic seizures, which were controlled by anti-epileptic drugs. Polymicrogyria in the right frontal operculum-perisylvian region was revealed by magnetic resonance imaging at 18 months old (Fig. 1E,F). He had an arterial septal defect and dysplastic tricuspid valve, but surgery was not required. Standard audiometric examinations, spinal X-ray, bone age, and G-banding karyotype were all normal.

The observed multisystem organ impairment suggested that the patient's phenotype might be caused by a chromosomal structural abnormality [Feuk et al., 2006]. We therefore performed a copy number analysis and detected a 1.4-Mb deletion at 21q22.11 (chr21 33,824,925–35,242,759 bp) but no other abnormal copy number variations. This deleted region includes 19 protein-coding RefSeq genes (*EVA1C, TCP10L, C21orf59, SYNJ1, PAXBP1, C21orf62, OLIG1, OLIG2, IFNAR2, IFNAR1, IL10RB, IFNGR2, TMEM50B, DNAJC28, GART, SON, DONSON, CRYZL1*, and *ITSN1*, according to the UCSC database as of July 2013). The deletion was confirmed by FISH to be de novo (Fig. 2).

## DISCUSSION

We present a Japanese patient with a de novo 1.4-Mb deletion at 21q22.11. To the best of our knowledge, at least 16 other reported patients share the deleted region and clinical manifestations with our patient (Table I) [Braddock and Carey, 1994; Orti et al., 1997; Albert, 2001; Yao et al., 2006; Hoyer et al., 2007; Beri-Dexheimer et al., 2008; Shinawi et al., 2008; Lyle et al., 2009; Katzaki et al., 2010; Lindstrand et al., 2010; Byrd et al., 2011; Click et al., 2011; Melis et al., 2011; Thevenon et al., 2011; Izumi et al., 2012]. Among the three described regions of partial monosomy 21, regions 2 and/or 1 may produce a more severe phenotype than that produced by region 3 [Lyle et al., 2009; van der Crabben et al., 2010; Roberson et al., 2011]. Therefore, all three regions (especially region 2) were carefully considered when we compared the phenotype–genotype correlation in those patients regardless of limited clinical information (Fig. 2A). Growth and developmental delays and microcephaly were observed in most of the patients (Table I). Among the 17 above cases, no identical deletions were detected, but the intersectin 1 gene (*ITSN1*, NM_003024.2) was commonly deleted or disrupted. There were also 12 patients with a non-overlapping 21q22 deletion, which may be useful for exclusion mapping (Fig. 2B). However, most of the non-overlapping deletion patients (10/11) also had

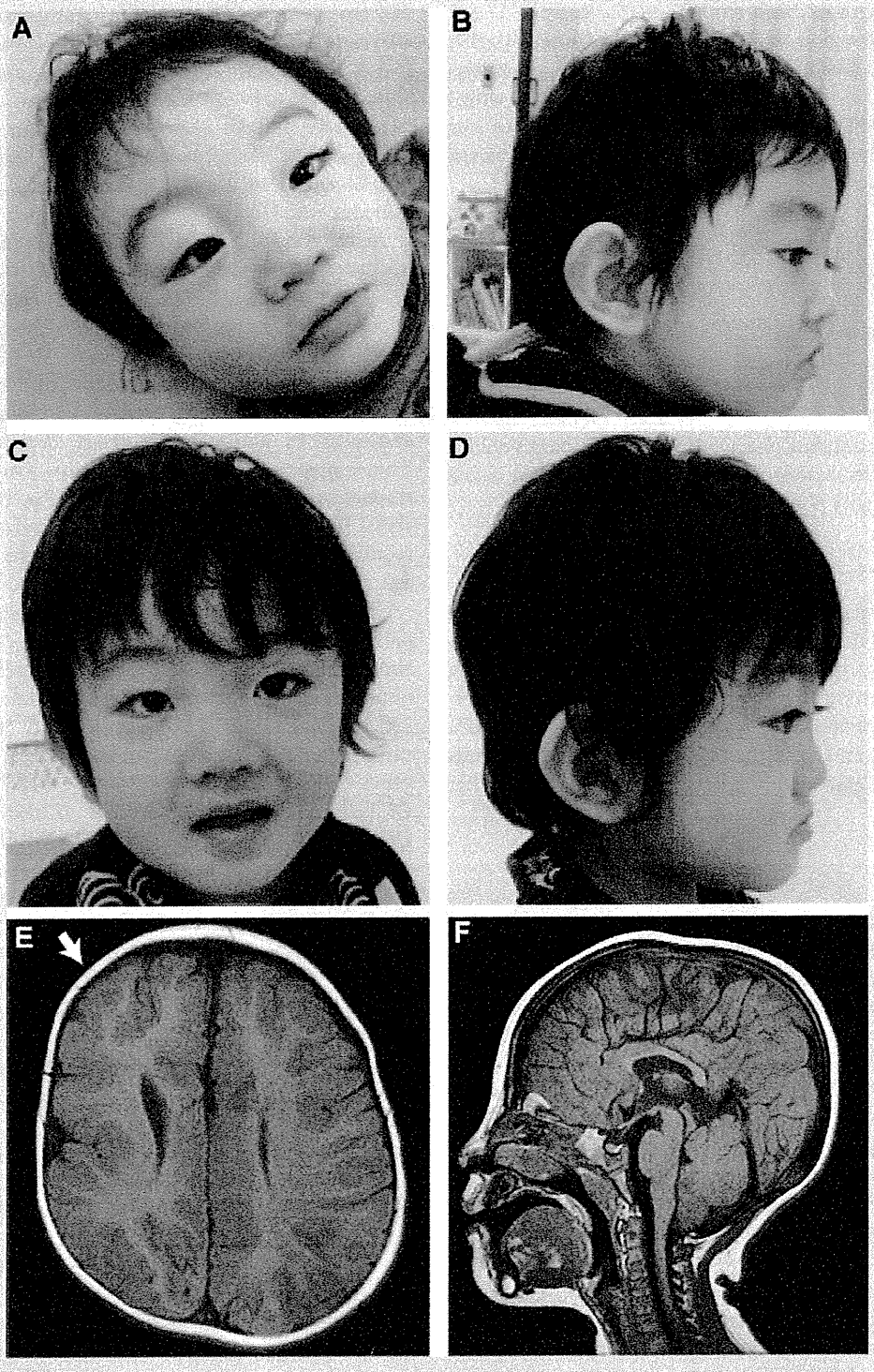


FIG. 1. Clinical features of the patient. A–D: Facial appearance of the patient at age 11 months (A), 18 months (B), and 22 months (C,D). He showed dysmorphic facial features, including iris coloboma and low-set ears. E,F: Brain magnetic resonance imaging of the patient at age 18 months. T1-weighted coronal (E) and sagittal (F) sections are shown. Polymicrogyria is seen in the right frontal operculum-perisylvian region (white arrow).

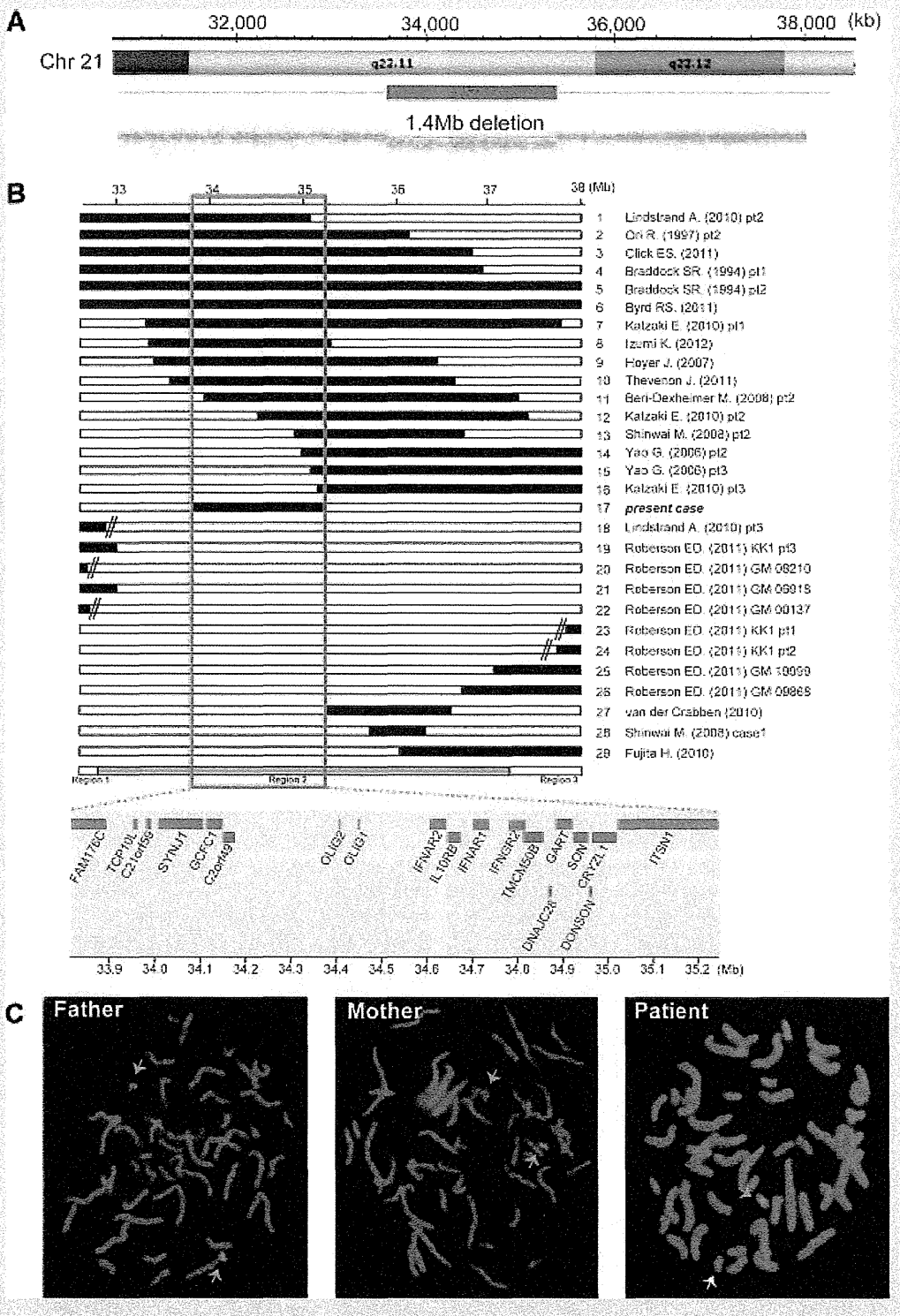


**FIG. 2. Cytogenetic studies on 21q22. A: Scheme of the deleted segment (red box) of chromosome 21 in the patient. B: The upper panel shows 16 previously reported patients sharing the region deleted in the patient, and 12 other patients with a non-overlapping deletion. For each individual, the normal and deleted regions are shown as white and black bars, respectively. The deleted region in the patient is shown as a red box and magnified in light green shadow. The bottom bar indicates regions 1, 2, and 3 as proposed in the literature. Nineteen protein-coding genes are located within this deleted region (shown at the bottom). The genomic position is based on the UCSC genome browser build 37 (hg19). C: Two-color FISH illustrating the de novo deletion of RP11-70F1 (white arrow) in the patient. Orange arrows indicate normal signals from RP11-626D11.**

TABLE I. Clinical Features of Patients With Deletion of 21q22.11 and/or the Flanking Region

| Case [ref.] | Deletion (Mb) | Sex | Low birth weight | Growth delay | Short stature | Microcephaly | Short neck | Eye anomalies | Low set ears | Down-turned corner of the mouth | Skeletal anomalies | Hypoplastic nails | Heart malformation | Developmental delay | Brain structural anomalies | Seizure | Hypotonus |
|---|---|---|---|---|---|---|---|---|---|---|---|---|---|---|---|---|---|
| 1. Lindstrand et al. [2010] pt2 | 23.13–35.07 | F | + | + | n.m. | n.m. | + | Hyperopia, coloboma | + | n.m. | + | n.m. | – | Severe | – | – | n.m. |
| 2. Orti et al. [1997], pt2 | 27.26–36.09 | F | + | + | n.m. | n.m. | n.m. | n.m. | n.m. | n.m. | n.m. | n.m. | n.m. | IQ < 10 | n.m. | n.m. | n.m. |
| 3. Click et al. [2011] | 23.64–36.85 | F | IUGR | + | n.m. | + | n.m. | Strabismus, tunica vasculosa lentis | + | n.m. | + | n.m. | TOF, DORV | + | – | – | + |
| 4. Braddock and Carey [1994], pt1 | 31.08–38.63 | F | + | + | + | + | n.m. | n.m. | + | + | + | n.m. | VSD | + | A/H | n.m. | + |
| 5. Braddock and Carey [1994], pt2 | 26.99–36.91 | F | + | + | + | + | + | n.m. | + | + | + | n.m. | – | + | A/H | n.m. | + |
| 6. Byrd et al. [2011] | 31.77–38.08 | F | + | + | n.m. | – | n.m. | Strabismus, epicanthal fold | + | + | + | n.m. | ASD | + | A/H | – | n.m. |
| 7. Katzaki et al. [2010], pt1 | 33.29–37.762 | F | + | + | + | + | n.m. | Strabismus | + | + | + | + | – | + | – | – | + |
| 8. Izumi et al. [2012] | 33.35–35.25 | F | + | + | + | – | n.m. | n.m. | – | + | + | n.m. | ASD, VSD, PDA | + | – | n.m. | + |
| 9. Hoyer et al. [2007] | 33.41–36.44 | n.m. | n.m. | + | + | – | n.m. | n.m. | n.m. | n.m. | n.m. | n.m. | – | + | n.m. | – | n.m. |
| 10. Thevenon et al. [2011] | 33.64–36.64 | M | + | + | + | + | + | Strabismus, microcornea, goniodysgenesis, hypermetropia | + | n.m. | + | n.m. | ASD, hypertrophic | + | Unformed cingulate gyri, A/H | + | + |
| 11. Beri-Dexheimer et al. [2008], pt2 | 33.93–37.33 | F | + | + | + | + | n.m. | Strabismus, enopthtalmia | – | + | – | n.m. | ASD | + | Increased size of lateral ventricles, P | – | + |
| 12. Katzaki et al. [2010], pt2 | 34.53–37.45 | M | + | + | + | + | n.m. | n.m. | + | + | + | + | – | + | A/H | + | n.m. |
| 13. Shinawi et al. [2008], pt2 | 34.91–36.73 | F | + | + | + | + | n.m. | Hypertelorism, epicanthal folds | n.m. | + | – | + | – | Global | A/H, delayed myelination | – | n.m. |
| 14. Yao et al. [2006], pt2 | 34.96/35.01 - qter | F | + | n.m. | n.m. | + | Webbed neck | + | – | n.m. | + | n.m. | + | Severe | Pacydyria, P, A/H, and other | + | + |
| 15. Yao et al. [2006], pt3 | ~35.08–47.18 | F | + | n.m. | n.m. | + | Webbed neck | + | Dysmorphic | n.m. | + | n.m. | + | Moderate | Pacydyria, P, A/H, and other | + | n.m. |
| 16. Katzaki et al. [2010], pt3 | 35.14–39.38 | F | + | n.m. | n.m. | + | n.m. | Strabismus | – | + | – | n.m. | ASD | + | – | + | n.m. |
| 17. Present case | 33.82–35.24 | M | – | + | + | + | + | Iris coloboma | + | + | – | + | ASD | + | P | + | + |
| 18. Lindstrand et al. [2010], pt3 | 15.37–29.34 | M | – | – | – | n.m. | n.m. | Astigmatis | n.m. | n.m. | n.m. | n.m. | Aortic stenosis | Mild | n.m. | – | n.m. |
| 19. Roberson et al. [2011], KK1 pt3 | 18.19–34.60 | F | n.m. | + | n.m. | n.m. | n.m. | Strabismus | n.m. | n.m. | n.m. | n.m. | TR | Prompt | – | n.m. | + |

*(Continued)*

TABLE I. (*Continued*)

| Case [ref.] | Deletion (Mb) | Sex | Low birth weight | Growth delay | Short stature | Microcephaly | Short neck | Eye anomalies | Low set ears | Down-turned corner of the mouth | Skeletal anomalies | Hypoplastic nails | Heart malformation | Developmental delay | Brain structural anomalies | Seizure | Hypotonus |
|---|---|---|---|---|---|---|---|---|---|---|---|---|---|---|---|---|---|
| 20. Roberson et al. [2011], GM08210 | 14.78–18.93 | F | + | + | + | + | n.m. | n.m. | + | n.m. | + | n.m. | n.m. | + | n.m. | n.m. | + |
| 21. Roberson et al. [2011], GM05918 | 16.35–33.67 | M | n.m. | n.m. | + | n.m. | n.m. | n.m. | + | + | + | n.m. | n.m. | Moderate | n.m. | n.m. | n.m. |
| 22. Roberson et al. [2011], GM00137 | 14.78–29.76 | M | n.m. | n.m. | n.m. | + | n.m. | Bilateral coloboma, ocular hypertelorism, bilateral epicanthal folds | + | + | + | n.m. | n.m. | Severe | n.m. | n.m. | n.m. |
| 23. Roberson et al. [2011], KK1 pt1 | 43.17–48.08 | M | n.m. | + | n.m. | n.m. | n.m. | Bilateral epicanthal folds, stellate iris, strabismus | n.m. | n.m. | + | n.m. | n.m. | Mild–moderate | – | n.m. | + |
| 24. Roberson et al. [2011], KK1 pt2 | 42.31–48.08 | M | n.m. | Over growth | n.m. | n.m. | – | Strabismus | – | n.m. | – | – | n.m. | Moderate | n.m. | n.m. | n.m. |
| 25. Roberson et al. [2011], GM19999 | 37.24–48.10 | F | IUGR | n.m. | n.m. | n.m. | n.m. | Cornea clouding | n.m. | n.m. | n.m. | n.m. | VSD | n.m. | n.m. | n.m. | n.m. |
| 26. Roberson et al. [2011], GM09868 | 36.76–48.10 | F | n.m. | n.m. | n.m. | n.m. | n.m. | n.m. | + | + | + | n.m. | n.m. | n.m. | n.m. | n.m. | n.m. |
| 27. van der Crabben et al. [2010] | 35.28–36.86 | M | n.m. | – | n.m. | – | n.m. | n.m. | n.m. | n.m. | n.m. | n.m. | – | – | n.m. | n.m. | n.m. |
| 28. Shinawi et al. [2008], pt1 | 35.87–36.59 | M | – | + | + | 5–10th centile | n.m. | Hypertelorism, almond-shaped | n.m. | n.m. | n.m. | n.m. | Great vessel transposition | Fine motor | – | – | n.m. |
| 29. Fujita et al. [2010] | 36.06–40.04 | M | IUGR | + | + | + | n.m. | Corneal opacity | n.m. | n.m. | n.m. | Thick toe nails | n.m. | Severe | – | n.m. | n.m. |

M, male; F, female; +, feature present; –, feature absent; n.m., not mentioned; TOF, tetralogy of Fallot; DORV, double outlet right ventricle; ASD, atrial septal defect; VSD, ventricular septal defect; PDA, patent ductus arteriosus; TR, tricuspid regurgitation; A/H, agenesis/hypoplasia of the corpus callosum; P, polymicrogyria.

mild-to-severe developmental delay; thus, there could be other genes related to developmental delay in these regions.

ITSN1 is a cytoplasmic membrane-associated protein that indirectly coordinates endocytic membrane traffic with the actin assembly machinery. It has been implicated in the pathogenesis of Down syndrome, Alzheimer disease, and potentially other neurodegenerative diseases [Hunter et al., 2011; Tsyba et al., 2011; Morderer et al., 2012]. The short isoform of *ITSN1* is expressed ubiquitously, while the long isoform shows neuron-specific expression [Pucharcos et al., 2001]. As ITSN1 acts as scaffold protein in endocytosis, its haploinsufficiency may damage brain tissues [van der Crabben et al., 2010]. A recent study of *Itsn1* homozygous mutant mice showed learning impairment, especially spatial learning deficits [Sengar et al., 2013]. Therefore, *ITSN1* deletion may be associated with intellectual developmental delay [van der Crabben et al., 2010].

Among 17 patients (Patients 1–17) in Table I, all (100%) had developmental delay. The minimal overlapping region was 35.14 to 35.24 Mb, containing part of only one protein-coding RefSeq gene, *ITSN1* (Fig. 2B). A non-overlapping patient (case 27 in Fig. 2B, Table I), with no *ITSN1* disruption, did not have developmental delay. This is consistent with *ITSN1* haploinsufficiency being involved in the developmental impairment.

Twelve of the 17 patients (70.6%; the 17 patients comprising the present patient plus the 16 patients with an overlapping deletion) showed microcephaly. The minimal region of overlap among them again maps to the region from 35.14 to 35.24 Mb, including part of *ITSN1*. Interestingly, homozygous *Itsn1* mutant mice have a smaller brain as a percentage of body mass compared with wild-type mice [Sengar et al., 2013]. Therefore, microcephaly may also result from *ITSN1* haploinsufficiency. In addition, 10 of the 17 patients (59%) shared various brain structural anomalies, including pachygyria, polymicrogyria, hypoplasia of the corpus callosum, subcortical white matter and cerebellum, and an enlarged ventricular system (Table I). The current patient also presented with microcephaly and partial polymicrogyria in the right frontal operculum-perisylvian region. The minimal region of overlap for brain structural anomalies was 35.08–35.24 Mb, which contains only *ITSN1* (Fig. 2B). *Itsn1*-null mice also showed agenesis of the corpus callosum [Sengar et al., 2013]. In 6 of the 10 patients with abnormal brain structures, seizures were observed. Brain structural abnormalities are known to be associated with seizures [Leventer et al., 2010; Tavyev Asher and Scaglia, 2012]; five of the six patients with seizures had polymicrogyria and/or hypoplasia of the corpus callosum (Table I).

In our case, the skeletal features were unremarkable, but 13 patients with an overlapping deletion had skeletal abnormalities. Regardless of inclusion and exclusion mapping (Fig. 2B), we were unable to list candidate genes related to skeletal phenotypes. We next focused the ocular phenotype, coloboma. Only two patients, including ours, exhibited coloboma, and the minimal region of overlap was large (33.38–35.07 Mb), harboring 19 protein-coding RefSeq genes. Therefore, we could not narrow down the gene(s) associated with coloboma. Similarly, the shortest overlapping region for heart malformation, including arterial septal defect, was also large (33.93–35.24 Mb) and contained 18 protein-coding RefSeq genes. It is well known that an extra copy of genes on chromosome 21 is associated with heart malformation. In particular, genes involved in cell adhesion may be associated with heart defects [Barlow et al., 2001; Mao et al., 2005], although this is not well understood.

In summary, we report on a patient with a de novo 1.4-Mb deletion at 21q22 presenting with developmental delay. Compared with other partial 21q22 deletion cases, our patient shows rather severe developmental delay with a variety of clinical phenotypes. We propose that haploinsufficiency of the *ITSN1* gene is strongly associated with developmental delay, microcephaly, and brain structural anomalies. Precise mapping of the genomic rearrangement together with careful literature review can yield useful information about genes associated with human phenotypes.

## ACKNOWLEDGMENTS

We thank the patient and his parents for participating in this work. We also thank Ms. Y. Yamashita for her technical assistance. This work was supported by research grants from the Ministry of Health, Labour and Welfare of Japan (H.S., N. Matsumoto, N. Miyake), the fund for Creation of Innovation Centers for Advanced Interdisciplinary Research Areas Program in the Project for Developing Innovation Systems (N. Matsumoto), the Strategic Research Program for Brain Sciences (N. Matsumoto), and a Grant-in-Aid for Scientific Research on Innovative Areas—(Transcription cycle)—from the Ministry of Education, Culture, Sports, Science and Technology of Japan (N. Matsumoto), a Grant-in-Aid for Scientific Research from the Japan Society for the Promotion of Science (N. Matsumoto), a Grant-in-Aid for Young Scientists from the Japan Society for the Promotion of Science (H.S., N. Miyake), the Takeda Science Foundation (N. Matsumoto, N. Miyake), the Yokohama Foundation for Advancement of Medical Science (N. Miyake), and the Hayashi Memorial Foundation for Female Natural Scientists (N. Miyake).

## REFERENCES

Albert S, editor. 2001. Catalog of unbalanced chromosomal aberrations in man. In: Chromosome 21, 2nd edition. Berlin, NY: Walter de Gruyter & Co. pp 807–817.

Barlow GM, Chen XN, Shi ZY, Lyons GE, Kurnit DM, Celle L, Spinner NB, Zackai E, Pettenati MJ, Van Riper AJ, Vekemans MJ, Mjaatvedt CH, Korenberg JR, 2001. Down syndrome congenital heart disease a narrowed region and a candidate gene. Genet Med 3:91–101.

Beri-Dexheimer M, Latger-Cannard V, Philippe C, Bonnet C, Chambon P, Roth V, Gregoire MJ, Bordigoni P, Lecompte T, Leheup B, Jonveaux P. 2008. Clinical phenotype of germline RUNX1 haploinsufficiency: From point mutations to large genomic deletions. Eur J Hum Genet 16:1014–1018.

Braddock SR, Carey JC. 1994. A new syndrome: Congenital thrombocytopenia, Robin sequence, agenesis of the corpus callosum, distinctive facies and developmental delay. Clin Dysmorphol 3:75–81.

Braddock SR, Schiffman JD, Sarah T, South ST, Carey JC. 2011. Braddock-Carey syndrome: A twenty year journey ends with a new microdeletion syndrome. 32nd Annual David W. Smith Workshop on Malformations and Morphogenesis, Lake Arrowhead, CA, USA.

Byrd RS, Zwerdling T, Moghaddam B, Pinter JD, Steinfeld MB. 2011. Monosomy 21q22.11-q22.13 presenting as a Fanconi anemia phenotype. Am J Med Genet Part A 155A:120–125.

Chen CP, Chern SR, Lee CC, Chen LF, Chin DT, Tzen CY, Wang W. 2003. Prenatal diagnosis of trisomy 18p and distal 21q22.3 deletion. Prenat Diagn 23:758–761.

Chettouh Z, Croquette MF, Delobel B, Gilgenkrants S, Leonard C, Maunoury C, Prieur M, Rethore MO, Sinet PM, Chery M, et al. 1995. Molecular mapping of 21 features associated with partial monosomy 21: Involvement of the APP-SOD1 region. Am J Hum Genet 57: 62–71.

Click ES, Cox B, Olson SB, Grompe M, Akkari Y, Moreau LA, Shimamura A, Sternen DL, Liu YJ, Leppig KA, Matthews DC, Parisi MA. 2011. Fanconi anemia-like presentation in an infant with constitutional deletion of 21q including the RUNX1 gene. Am J Med Genet Part A 155A:1673–1679.

Courtens W, Petersen MB, Noel JC, Flament-Durand J, Van Regemorter N, Delneste D, Cochaux P, Verschraegen-Spae MR, Van Roy N, Speleman F, et al. 1994. Proximal deletion of chromosome 21 confirmed by in situ hybridization and molecular studies. Am J Med Genet 51:260–265.

Enjoji M, Yanai N. 1961. Analytic test for development in infancy and childhood. Pediatr Int 4:2–6.

Feuk L, Carson AR, Scherer SW. 2006. Structural variation in the human genome. Nat Rev Genet 7:85–97.

Fujita H, Torii C, Kosaki R, Yamaguchi S, Kudoh J, Hayashi K, Takahashi T, Kosaki K. 2010. Microdeletion of the Down syndrome critical region at 21q22. Am J Med Genet Part A 152A:950–953.

Hoyer J, Dreweke A, Becker C, Gohring I, Thiel CT, Peippo MM, Rauch R, Hofbeck M, Trautmann U, Zweier C, Zenker M, Huffmeier U, Kraus C, Ekici AB, Ruschendorf F, Nurnberg P, Reis A, Rauch A. 2007. Molecular karyotyping in patients with mental retardation using 100K single-nucleotide polymorphism arrays. J Med Genet 44:629–636.

Hunter MP, Nelson M, Kurzer M, Wang X, Kryscio RJ, Head E, Pinna G, O'Bryan JP. 2011. Intersectin 1 contributes to phenotypes in vivo: Implications for Down's syndrome. Neuroreport 22:767–772.

Huret JL, Leonard C, Chery M, Philippe C, Schafei-Benaissa E, Lefaure G, Labrune B, Gilgenkrantz S. 1995. Monosomy 21q: Two cases of del(21q) and review of the literature. Clin Genet 48:140–147.

Izumi K, Brooks SS, Feret HA, Zackai EH. 2012. 1.9 Mb microdeletion of 21q22.11 within Braddock-Carey contiguous gene deletion syndrome region: Dissecting the phenotype. Am J Med Genet Part A 158A:1535–1541.

Katzaki E, Morin G, Pollazzon M, Papa FT, Buoni S, Hayek J, Andrieux J, Lecerf L, Popovici C, Receveur A, Mathieu-Dramard M, Renieri A, Mari F, Philip N. 2010. Syndromic mental retardation with thrombocytopenia due to 21q22.11q22.12 deletion: Report of three patients. Am J Med Genet Part A 152A:1711–1717.

Leventer RJ, Jansen A, Pilz DT, Stoodley N, Marini C, Dubeau F, Malone J, Mitchell LA, Mandelstam S, Scheffer IE, Berkovic SF, Andermann F, Andermann E, Guerrini R, Dobyns WB. 2010. Clinical and imaging heterogeneity of polymicrogyria: A study of 328 patients. Brain 133: 1415–1427.

Lindstrand A, Malmgren H, Sahlen S, Schoumans J, Nordgren A, Ergander U, Holm E, Anderlid BM, Blennow E. 2010. Detailed molecular and clinical characterization of three patients with 21q deletions. Clin Genet 77:145–154.

Lyle R, Bena F, Gagos S, Gehrig C, Lopez G, Schinzel A, Lespinasse J, Bottani A, Dahoun S, Taine L, Doco-Fenzy M, Cornillet-Lefebvre P, Pelet A, Lyonnet S, Toutain A, Colleaux L, Horst J, Kennerknecht I, Wakamatsu N, Descartes M, Franklin JC, Florentin-Arar L, Kitsiou S, Ait Yahya-Graison E, Costantine M, Sinet PM, Delabar JM, Antonarakis SE. 2009. Genotype-phenotype correlations in Down syndrome identified by array CGH in 30 cases of partial trisomy and partial monosomy chromosome 21. Eur J Hum Genet 17:454–466.

Mao R, Wang X, Spitznagel EL Jr, Frelin LP, Ting JC, Ding H, Kim JW, Ruczinski I, Downey TJ, Pevsner J. 2005. Primary and secondary transcriptional effects in the developing human Down syndrome brain and heart. Genome Biol 6:R107.

Melis D, Genesio R, Cappuccio G, MariaGinocchio V, Casa RD, Menna G, Buffardi S, Poggi V, Leszle A, Imperati F, Carella M, Izzo A, Del Giudice E, Nitsch L, Andria G. 2011. Mental retardation, congenital heart malformation, and myelodysplasia in a patient with a complex chromosomal rearrangement involving the critical region 21q22. Am J Med Genet Part A 155A:1697–1705.

Morderer D, Nikolaienko O, Skrypkina I, Cherkas V, Tsyba L, Belan P, Rynditch A. 2012. Endocytic adaptor protein intersectin 1 forms a complex with microtubule stabilizer STOP in neurons. Gene 505: 360–364.

Oegema R, de Klein A, Verkerk AJ, Schot R, Dumee B, Douben H, Eussen B, Dubbel L, Poddighe PJ, van der Laar I, Dobyns WB, van der Spek PJ, Lequin MH, de Coo IF, de Wit MC, Wessels MW, Mancini GM. 2010. Distinctive phenotypic abnormalities associated with submicroscopic 21q22 deletion including DYRK1A. Mol Syndromol 1:113–120.

Orti R, Mégarbane A, Maunoury C, Van Broeckhoven C, Sinet PM, Delabar JM. 1997. High-resolution physical mapping of a 6.7-Mb YAC contig spanning a region critical for the monosomy 21 phenotype in 21q21.3–q22.1. Genomics 43:25–33.

Pucharcos C, Casas C, Nadal M, Estivill X, de la Luna S. 2001. The human intersectin genes and their spliced variants are differentially expressed. Biochim Biophys Acta 1521:1–11.

Roberson ED, Wohler ES, Hoover-Fong JE, Lisi E, Stevens EL, Thomas GH, Leonard J, Hamosh A, Pevsner J. 2011. Genomic analysis of partial 21q monosomies with variable phenotypes. Eur J Hum Genet 19:235–238.

Sengar AS, Ellegood J, Yiu AP, Wang H, Wang W, Juneja SC, Lerch JP, Josselyn SA, Henkelman RM, Salter MW, Egan SE. 2013. Vertebrate intersectin1 is repurposed to facilitate cortical midline connectivity and higher order cognition. J Neurosci 33:4055–4065.

Shinawi M, Erez A, Shardy DL, Lee B, Naeem R, Weissenberger G, Chinault AC, Cheung SW, Plon SE. 2008. Syndromic thrombocytopenia and predisposition to acute myelogenous leukemia caused by constitutional microdeletions on chromosome 21q. Blood 112:1042–1047.

Tavyev Asher YJ, Scaglia F. 2012. Molecular bases and clinical spectrum of early infantile epileptic encephalopathies. Eur J Med Genet 55:299–306.

Theodoropoulos DS, Cowan JM, Elias ER, Cole C. 1995. Physical findings in 21q22 deletion suggest critical region for 21q- phenotype in q22. Am J Med Genet 59:161–163.

Thevenon J, Callier P, Thauvin-Robinet C, Mejean N, Falcon-Eicher S, Maynadie M, de Maistre E, Bidot S, Huet F, Beri-Dexheimer M, Jonveaux P, Mugneret F, Faivre L. 2011. De novo 21q22.1q22.2 deletion including RUNX1 mimicking a congenital infection. Am J Med Genet Part A 155A:126–129.

Tsyba L, Nikolaienko O, Dergai O, Dergai M, Novokhatska O, Skrypkina I, Rynditch A. 2011. Intersectin multidomain adaptor proteins: Regulation of functional diversity. Gene 473:67–75.

van der Crabben S, van Binsbergen E, Ausems M, Poot M, Bierings M, Buijs A. 2010. Constitutional RUNX1 deletion presenting as non-syndromic thrombocytopenia with myelodysplasia: 21q22 ITSN1 as a candidate gene in mental retardation. Leuk Res 34:e8–e12.

Yao G, Chen XN, Flores-Sarnat L, Barlow GM, Palka G, Moeschler JB, McGillivray B, Morse RP, Korenberg JR. 2006. Deletion of chromosome 21 disturbs human brain morphogenesis. Genet Med 8:1–7.

Journal of Human Genetics (2014), 1–4

www.nature.com/jhg

SHORT COMMUNICATION

# A novel homozygous *YARS2* mutation causes severe myopathy, lactic acidosis, and sideroblastic anemia 2

Junya Nakajima[1,2], Tuba F Eminoglu[3], Goksel Vatansever[4], Mitsuko Nakashima[1], Yoshinori Tsurusaki[1], Hirotomo Saitsu[1], Hisashi Kawashima[2], Naomichi Matsumoto[1] and Noriko Miyake[1]

**Mitochondrial diseases are associated with defects of adenosine triphosphate production and energy supply to organs as a result of dysfunctions of the mitochondrial respiratory chain. Biallelic mutations in the *YARS2* gene encoding mitochondrial tyrosyl-tRNA synthetase cause myopathy, lactic acidosis, and sideroblastic anemia 2 (MLASA2), a type of mitochondrial disease. Here, we report a consanguineous Turkish family with two siblings showing severe metabolic decompensation including recurrent hypoglycemia, lactic acidosis, and transfusion-dependent anemia. Using whole-exome sequencing of the proband and his parents, we identified a novel *YARS2* mutation (c.1303A>G, p.Ser435Gly) that was homozygous in the patient and heterozygous in his parents. This mutation is located at the ribosomal protein S4-like domain of the gene, while other reported *YARS2* mutations are all within the catalytic domain. Interestingly, the proband showed more severe symptoms and an earlier onset than previously reported patients, suggesting the functional importance of the S4-like domain in tyrosyl-tRNA synthetase.**
*Journal of Human Genetics* advance online publication, 16 January 2014; doi:10.1038/jhg.2013.143

**Keywords:** mitochondria; myopathy, lactic acidosis and sideroblastic anemia 2; tyrosyl-tRNA synthetase; whole-exome sequencing; *YARS2*

Aminoacyl-tRNA synthetases (ARSs) are essential enzymes that attach specific amino acids to the corresponding tRNAs (aminoacylation). Among a total of 36 human ARSs , YARS (tyrosyl-tRNA synthetase) and YARS2 (tyrosyl-tRNA synthetase 2; mitochondrial ARSs are nominally numbered '2') catalyze the binding of tyrosine to their cognate cytoplasmic and mitochondrial tRNAs, respectively.[1] YARS2 is encoded by the nuclear gene *YARS2* (NM_001040436.2) at 12p11.21. ARSs do not complement each other. Mutations in 11 of 17 mitochondrial ARS genes cause a wide variety of diseases according to PubMed (http://www.ncbi.nlm.nih.gov/pubmed) and the Human Genome Mutation Database professional (https://portal.biobase-international.com/hgmd/pro/start.php).[2] For example, biallelic mutations in *DARS2*, *RARS2*, *FARS2*, and *AARS2* cause leukoencephalopathy with brain stem and spinal cord involvement and lactate elevation (MIM#611105), pontocerebellar hypoplasia, type 6 (MIM#611523), combined oxidative phosphorylation deficiency 14 (MIM#614946) showing fatal epileptic encephalopathy, and combined oxidative phosphorylation deficiency 8 (MIM#614096) presenting with lethal infantile cardiomyopathy, respectively.[3–6] YARS2 defects also cause loss of mitochondrial tyrosyl-tRNA (mt-tRNA$^{Tyr}$) leading to the failure of protein production in mitochondria.[1,7] *YARS2* mutations cause myopathy, lactic acidosis, and sideroblastic anemia 2 (MLASA2, MIM#613561),[8–10] which is an autosomal recessive disorder characterized by relatively mild symptoms of oxidative phosphorylation defects including progressive muscle weakness and sideroblastic anemia.[8–10] To our knowledge, only four families with *YARS2* mutations have thus far been reported.[8–10]

The proband (II-4) is the fourth child of healthy Turkish parents who are first cousins (Figure 1a). He was born by normal delivery at 39 weeks of gestation with a birth weight of 2900 g. The pregnancy and birth history were uneventful. On the 4th day of life, he showed poor feeding, tachypnea (80 breaths/min), metabolic acidosis (pH 7.14, $PCO_2$ 26.7 mm Hg, $HCO_3^-$ 5.1 mmol l$^{-1}$, base excess 18.6 mmol l$^{-1}$), and hyperlactacidemia (lactate 3.74 mmol l$^{-1}$) while carnitine, acylcarnitine, and quantitative amino acid analysis of plasma and urine were normal. Following a few weeks without any symptoms after the discharge, he suffered the rapid progression of normocytic anemia and recurrent metabolic decompensation including lactic acidosis, ketosis, and hyperammonemia (Supplementary Table 1). At 7 weeks of age, red blood cells were transfused due to the rapidly progressive anemia (Supplementary Table 2). At 2 months of age, he showed axial hypotonia. His ophthalmologic examination at this age was normal, although a brain magnetic resonance imaging scan showed thinning of the corpus callosum with normal progress of

[1]Department of Human Genetics, Yokohama City University Graduate School of Medicine, Yokohama, Japan; [2]Department of Pediatrics, Tokyo Medical University, Shinjuku, Japan; [3]Department of Pediatric Metabolism, Ankara University School of Medicine, Ankara, Turkey and [4]Department of Pediatrics, Ankara University School of Medicine, Ankara, Turkey
Correspondence: Dr N Miyake, Department of Human Genetics, Yokohama City University Graduate School of Medicine, Fukuura 3-9, Kanazawa-ku, Yokohama, Kanagawa 236-0004, Japan.
E-mail: nmiyake@yokohama-cu.ac.jp
Received 16 November 2013; revised 17 December 2013; accepted 17 December 2013

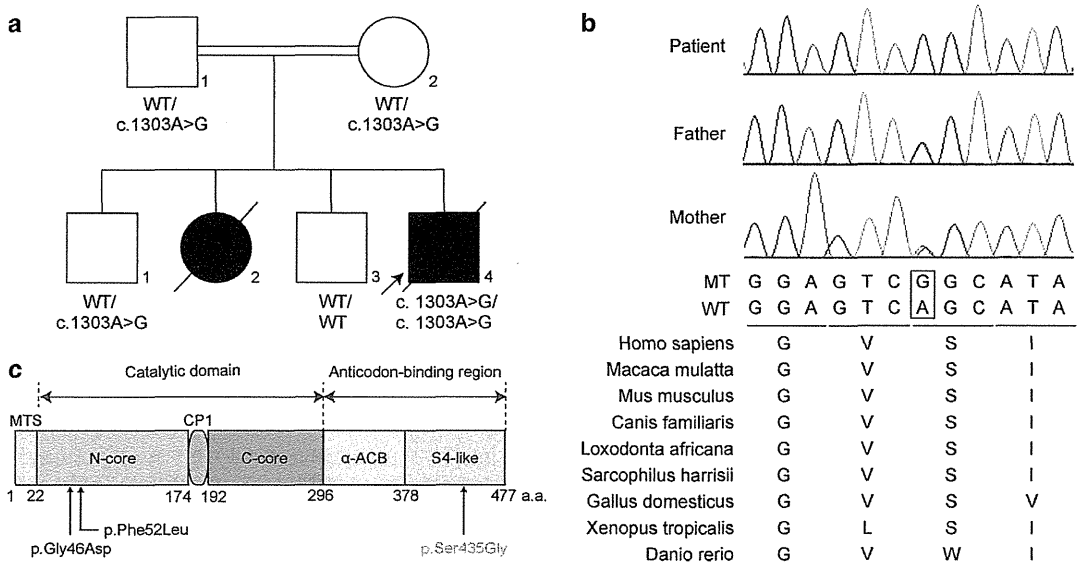


**Figure 1** Genetic analysis of the *YARS* mutation in this pedigree. (**a**) Pedigree tree of the affected family and mutation segregation. (**b**) Electropherograms of the *YARS2* mutation (c.1303A>G). The mutated base is marked by a square. Evolutionary conservation is shown at the bottom. MT, mutant allele; WT, wild type allele (**c**) Schema of YARS2 protein with mutational localization. The patient's mutation is colored in red below the diagram of the protein, while previously reported mutations (p.Gly46Asp and p.Phe52Leu) are in black. MTS, mitochondrial target sequence; N-core and C-core, N and C part of the catalytic domain, respectively; CP1, connective peptide; α-ACB, α-helical anticodon-binding domain; S4-like, ribosomal protein S4-like protein; a.a., amino acid.

myelination. An echo cardiogram revealed hypertrophy of the interventricular septum and left ventricle. The presence of proteinuria and hypercalciuria may indicate proximal renal tubulopathy (Supplementary Table 3). The glomerular filtration rate and serum levels of calcium, phosphate and vitamin D were within normal range. Although 4OH-phenyllactate and 4OH-phenylpyruvate were elevated, the transaminase level was within normal range. He was admitted to the hospital total of five times because of episodic metabolic decompensation, while there were no obvious triggering factors like infection.

During the episodic metabolic decompensation, serum lactate, pyruvate, the lactate/pyruvate ratio, ketone bodies, Krebs cycle intermediates, ammonia and creatine kinase levels were all increased. Plasma amino acid analysis revealed remarkably high alanine levels (Supplementary Table 1). He was treated with supportive therapies including the intravenous infusion of glucose ($10\,mg\,kg^{-1}\,min^{-1}$) and sodium bicarbonate according to the calculation of $HCO3^-$ deficit ($0.5 \times$ body weight (kg) $\times$ 24 h-serum $HCO3^-$ (mEq/l)), and responded promptly within one hour after starting the therapy. As a defect of the mitochondrial respiratory chain (MRC) was suspected, he was treated with sodium dichloroacetate ($50\,mg\,kg^{-1}\,day^{-1}$), coenzyme $Q_{10}$, carnitine, biotin, and riboflavin. Unfortunately, he died at the age of 3 months from a cardiopulmonary arrest that occurred during a metabolic decompensation. The other affected sib (II-2) died at the age of 2 days following a similar clinical course to the proband. Unfortunately, detailed clinical information about this patient was unavailable.

To identify the genetic cause of their condition, we performed whole-exome sequencing on the proband (II-4) and his parents (I-1 and I-2) as described in Supplementary Methods. This study was approved by the institutional review board of Yokohama City University School of Medicine. As two of the four children from healthy parents were affected, we hypothesized that the disorder was an autosomal recessive disease and focused on homozygous variants of the WES data. After excluding synonymous variants and variants registered in dbSNP137, ESP6500, and our in-house database (exome data of 408 individuals), five homozygous variants remained (Supplementary Tables 4, 5). As four variants predicted as 'benign' by PolyPhen-2[11] and/or 'polymorphism' by MutationTaster[12] were excluded, only one homozygous missense mutation, c.1303A>G, p.Ser435Gly, in exon 5 of the *YARS2* gene was highlighted (Supplementary Table 5), which is known to cause MLASA2. Sanger sequencing revealed that only proband had homozygous *YARS2* mutation while the parents and unaffected sibs had a heterozygous one (Figures 1a and b). HomozygosityMapper[13] (http://www.homozygositymapper.org/) confirmed that this mutation was located within a 3.5 Mb homozygous stretch.

Interestingly, two affected patients in this study showed more severe clinical phenotypes than previously reported patients with MLASA2,[8–10] including recurrent metabolic decompensation, proximal renal tubulopathy, and brain abnormalities which are rarely seen in MLASA2 patients,[8,9,14] (Table 1, Supplementary Table 6). Early onset severe progressive anemia necessitating a blood transfusion was common to both our patient and the previously reported MLASA2 patients; this is most likely a result of the severe metabolic impairment of erythropoiesis. Unfortunately, we were unable to perform a bone marrow aspirate and a peripheral blood smear test to determine whether our patients had sideroblastic anemia because of their rapid deterioration.

Human YARS2 has a catalytic domain and an anticodon-binding region (Figure 1c). This anticodon-binding region consists of an α-helical anticodon-binding domain and a ribosomal protein S4-like domain (S4-like domain).[15] The S4-like domain is essential to recognize tRNA, and is evolutionarily well conserved from

**Table 1 Phenotypes of Patients with *YARS2* Mutations**

| | | Riley *et al.* | | | | |
|---|---|---|---|---|---|---|
| | Proband | 1[a] | 2[a] | 3 | Sasarman *et al.* | Shahni *et al.* |
| Ethnicity | Turkish | Lebanese | Lebanese | Lebanese | Lebanese | Lebanese |
| Sex | male | male | female | female | male | male |
| Gene mutation[b] | c.1303A>G | c.156C>G | c.156C>G | c.156C>G | c.137G>A | c.156C>G |
| Amino acid change | p.Ser435Gly | p.Phe52Leu | p.Phe52Leu | p.Phe52Leu | p.Gly46Asp | p.Phe52Leu |
| Onset | neonate | 10 weeks | infancy | infancy | n.m | 1 year |
| CNS and Neurology | hypoplastic corpus callosum | lethargy, normal cognition | normal cognition | normal cognition | normal | lethargy |
| Heart | HCM | HCM | n.m. | n.m. | n.m. | HCM |
| Kidney | renal tubulopathy | n.m. | n.m. | n.m. | n.m. | n.m. |
| Endocrine systems | hypoglycemia | n.m. | n.m. | n.m. | n.m. | n.m. |
| Skeletal muscle | weakness | weakness | weakness | mild weakness | mild weakness | muscle weakness |
| *Myopathy* | | | | | | |
| onset | neonate | toddler | infancy | infancy | n.m. | n.m. |
| severity | hypotonia,no head control | wheelchair at 17 years old | unable to walk 20 mat 16 years old | mild | mild | nocturnal BiPAP at 12.5 years old |
| *Anemia* | | | | | | |
| onset | 6 weeks | 10 weeks | infancy | 7 years | 31 years | 1 year |
| type | n.a. | sideroblastic | sideroblastic | sideroblastic | sideroblastic | sideroblastic |
| Blood transfusion | yes | yes | yes | yes | n.m. | yes |
| Others | diseased at 3 months | failure to thrive | failure to thrive | n.m. | n.m. | neutropenia |

Abbreviations: BiPAP, biphasic positive airway pressure; CNS, central nervous system; HCM, hypertrophic cardiomyopathy; n.a., not assayed; n.m., not mentioned; RTA, renal tubular acidosis.
[a]From the same family.
[b]All were homozygous mutations.

eubacteria to humans.[16,17] The mutation in our patient was located in the S4-like domain whereas all other previously reported *YARS2* mutations were in the catalytic domain (Figure 1c).[8–10] The difference of mutation location may explain the clinical differences among the patients. Furthermore, the mutated amino acid serine 435 is highly conserved from frog to human (Figure 1b). The change from a hydrophilic serine to a hydrophobic glycine residue might alter the protein static structure and impair the physiological function of YARS2.[18] Thus, an abnormal S4-like domain would impair the tyrosylation of mitochondrial tRNA resulted in MRC dysfunction.

In this study, WES technique appears to be the powerful method, especially for suspected mitochondrial diseases showing various clinical phenotypes. This is because the involvement of many mutant genes in MRC disorders hampers regular Sanger sequencing of candidate genes,[19,20] and biopsies and enzymological analysis of affected organs may be difficult because of the severity and rapid progression of the disease.

## ACKNOWLEDGEMENTS

We thank the patient and his family for participating in this work. We also thank Ms S Sugimoto and K Takabe for technical assistance. This work was supported by research grants from the Ministry of Health, Labour and Welfare (N. Matsumoto, N. Miyake), the fund for Creation of Innovation Centers for Advanced Interdisciplinary Research Areas Program in the Project for Developing Innovation Systems from the Ministry of Education, Culture, Sports, Science and Technology (N. Matsumoto), the Strategic Research Program for Brain Sciences (N. Matsumoto), a Grant-in-Aid for Scientific Research on Innovative Areas-(Transcription cycle)-from the Ministry of Education, Culture, Sports, Science and Technology of Japan (N. Matsumoto), a Grant-in-Aid for Scientific Research from the Japan Society for the Promotion of Science (H. Saitsu, N. Matsumoto, N. Miyake), the Takeda Science Foundation (N. Matsumoto, N. Miyake), and the Hayashi Memorial Foundation for Female Natural Scientists (N. Miyake).

1 Antonellis, A. & Green, E. D. The role of aminoacyl-tRNA synthetases in genetic diseases. *Annu. Rev. Genomics Hum. Genet.* **9,** 87–107 (2008).
2 Stenson, P. D., Mort, M., Ball, E. V., Shaw, K., Phillips, A. D. & Cooper, D. N. The Human Gene Mutation Database: building a comprehensive mutation repository for clinical and molecular genetics, diagnostic testing and personalized genomic medicine. *Hum. Genet.* (e-pub ahead of print 28 Sep 2013; doi: 10.1007/s00439-013-1358-4).
3 Scheper, G. C., van der Klok, T., van Andel, R. J., van Berkel, C. G., Sissler, M., Smet, J. *et al.* Mitochondrial aspartyl-tRNA synthetase deficiency causes leukoencephalopathy with brain stem and spinal cord involvement and lactate elevation. *Nat. Genet.* **39,** 534–539 (2007).
4 Edvardson, S., Shaag, A., Kolesnikova, O., Gomori, J. M., Tarassov, I., Einbinder, T. *et al.* Deleterious mutation in the mitochondrial arginyl-transfer RNA synthetase gene is associated with pontocerebellar hypoplasia. *Am. J. Hum. Genet.* **81,** 857–862 (2007).
5 Gotz, A., Tyynismaa, H., Euro, L., Ellonen, P., Hyotylainen, T., Ojala, T. *et al.* Exome sequencing identifies mitochondrial alanyl-tRNA synthetase mutations in infantile mitochondrial cardiomyopathy. *Am. J. Hum. Genet.* **88,** 635–642 (2011).
6 Elo, J. M., Yadavalli, S. S., Euro, L., Isohanni, P., Gotz, A., Carroll, C. J. *et al.* Mitochondrial phenylalanyl-tRNA synthetase mutations underlie fatal infantile Alpers encephalopathy. *Hum. Mol. Genet.* **21,** 4521–4529 (2012).
7 DiMauro, S. & Schon, E. A. Mitochondrial respiratory-chain diseases. *N. Engl. J. Med.* **348,** 2656–2668 (2003).
8 Sasarman, F., Nishimura, T., Thiffault, I. & Shoubridge, E. A. A novel mutation in YARS2 causes myopathy with lactic acidosis and sideroblastic anemia. *Hum. Mutat.* **33,** 1201–1206 (2012).
9 Riley, L. G., Cooper, S., Hickey, P., Rudinger-Thirion, J., McKenzie, M., Compton, A. *et al.* Mutation of the mitochondrial tyrosyl-tRNA synthetase gene, YARS2, causes myopathy, lactic acidosis, and sideroblastic anemia–MLASA syndrome. *Am. J. Hum. Genet.* **87,** 52–59 (2010).
10 Shahni, R., Wedatilake, Y., Cleary, M. A., Lindley, K. J., Sibson, K. R. & Rahman, S. A distinct mitochondrial myopathy, lactic acidosis and sideroblastic anemia (MLASA) phenotype associates with YARS2 mutations. *Am. J. Med. Genet. A* **161,** 2334–2338 (2013).
11 Adzhubei, I. A., Schmidt, S., Peshkin, L., Ramensky, V. E., Gerasimova, A., Bork, P. *et al.* A method and server for predicting damaging missense mutations. *Nat. Methods* **7,** 248–249 (2010).

12 Schwarz, J. M., Rodelsperger, C., Schuelke, M. & Seelow, D. MutationTaster evaluates disease-causing potential of sequence alterations. *Nat. Methods* **7**, 575–576 (2010).
13 Seelow, D., Schuelke, M., Hildebrandt, F. & Nurnberg, P. HomozygosityMapper–an interactive approach to homozygosity mapping. *Nucleic Acids Res.* **37**, W593–599 (2009).
14 Inbal, A., Avissar, N., Shaklai, M., Kuritzky, A., Schejter, A., Ben-David, E. *et al.* Myopathy, lactic acidosis, and sideroblastic anemia: a new syndrome. *Am. J. Med. Genet.* **55**, 372–378 (1995).
15 Bonnefond, L., Fender, A., Rudinger-Thirion, J., Giege, R., Florentz, C. & Sissler, M. Toward the full set of human mitochondrial aminoacyl-tRNA synthetases: characterization of AspRS and TyrRS. *Biochemistry* **44**, 4805–4816 (2005).
16 Yaremchuk, A., Kriklivyi, I., Tukalo, M. & Cusack, S. Class I tyrosyl-tRNA synthetase has a class II mode of cognate tRNA recognition. *EMBO J.* **21**, 3829–3840 (2002).
17 Guijarro, J. I., Pintar, A., Prochnicka-Chalufour, A., Guez, V., Gilquin, B., Bedouelle, H. *et al.* Structure and dynamics of the anticodon arm binding domain of Bacillus stearothermophilus Tyrosyl-tRNA synthetase. *Structure* **10**, 311–317 (2002).
18 Grantham, R. Amino acid difference formula to help explain protein evolution. *Science* **185**, 862–864 (1974).
19 Tucker, E. J., Compton, A. G. & Thorburn, D. R. Recent advances in the genetics of mitochondrial encephalopathies. *Curr. Neurol. Neurosci. Rep.* **10**, 277–285 (2010).
20 Bernier, F. P., Boneh, A., Dennett, X., Chow, C. W., Cleary, M. A. & Thorburn, D. R. Diagnostic criteria for respiratory chain disorders in adults and children. *Neurology* **59**, 1406–1411 (2002).

Supplementary Information accompanies the paper on Journal of Human Genetics website (http://www.nature.com/jhg)

BRIEF COMMUNICATION

# *PIGO* mutations in intractable epilepsy and severe developmental delay with mild elevation of alkaline phosphatase levels

*Kazuyuki Nakamura, †Hitoshi Osaka, ‡Yoshiko Murakami, †Rie Anzai, *Kiyomi Nishiyama, *Hirofumi Kodera, *Mitsuko Nakashima, *Yoshinori Tsurusaki, *Noriko Miyake, ‡Taroh Kinoshita, *Naomichi Matsumoto, and *Hirotomo Saitsu

*Epilepsia*, 55(2):e13–e17, 2014
doi: 10.1111/epi.12508

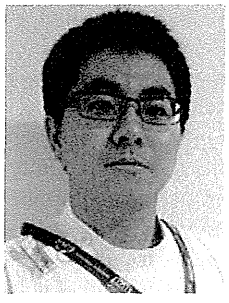

**Kazuyuki Nakamura** is a pediatric neurologist, and researches for epilepsy and brain malformation.

SUMMARY

**Aberrations in the glycosylphosphatidylinositol (GPI)–anchor biosynthesis pathway constitute a subclass of congenital disorders of glycosylation, and mutations in seven genes involved in this pathway have been identified. Among them, mutations in *PIGV* and *PIGO*, which are involved in the late stages of GPI-anchor synthesis, and *PGAP2*, which is involved in fatty-acid GPI-anchor remodeling, are all causative for hyperphosphatasia with mental retardation syndrome (HPMRS). Using whole exome sequencing, we identified novel compound heterozygous *PIGO* mutations (c.389C>A [p.Thr130Asn] and c.1288C>T [p.Gln430*]) in two siblings, one of them having epileptic encephalopathy. GPI-anchored proteins (CD16 and CD24) on blood granulocytes were slightly decreased compared with a control and his mother. Our patients lacked the characteristic features of HPMRS, such as facial dysmorphology (showing only a tented mouth) and hypoplasia of distal phalanges, and had only a mild elevation of serum alkaline phosphatase (ALP). Our findings therefore expand the clinical spectrum of GPI-anchor deficiencies involving *PIGO* mutations to include epileptic encephalopathy with mild elevation of ALP.**

KEY WORDS: **Congenital disorders of glycosylation, Epileptic encephalopathy, Glycosylphosphatidylinositol anchors, *PIGO*.**

More than 100 mammalian cell-surface proteins are anchored to the plasma membrane by the addition of glycosylphosphatidylinositol (GPI) to their C-termini. More than 20 genes are involved in the GPI-anchor biosynthesis pathway[1,2] of which 7 are mutated in GPI-anchor deficiencies, a subclass of congenital glycosylation disorders, in association with neurologic impairments.[3–7] Among them, mutations in *PIGV*, *PIGO* (both are involved in the last step of GPI-anchor synthesis), and *PGAP2* (involved in fatty-acid GPI-anchor remodeling) have been identified in patients with hyperphosphatasia with mental retardation syndrome (HPMRS), also known as Mabry syndrome.[3–8]

*PIGO* encodes GPI ethanolamine phosphate transferase 3, which is also known as phosphatidylinositol-glycan biosynthesis class O. To date, only three HPMRS families with compound heterozygous mutations in *PIGO* have been reported. In this study, we performed whole exome sequencing of a Japanese family containing two affected siblings, one of them having epileptic encephalopathy, and identified novel *PIGO* mutations that expand the clinical spectrum of *PIGO* abnormalities to include epileptic encephalopathy.

Accepted November 6, 2013; Early View publication January 13, 2014.
*Department of Human Genetics, Yokohama City University Graduate School of Medicine, Yokohama, Japan; †Division of Neurology, Clinical Research Institute, Kanagawa Children's Medical Center, Yokohama, Japan; and ‡Research Institute for Microbial Diseases and World Premier International Immunology Frontier Research Center, Osaka University, Osaka, Japan

Address correspondence to Hirotomo Saitsu, Department of Human Genetics, Yokohama City University Graduate School of Medicine, 3-9 Fukuura, Kanazawa-ku, Yokohama 236-0004, Japan. E-mail: hsaitsu@yokohama-cu.ac.jp

Wiley Periodicals, Inc.

## Methods

### DNA samples and subjects

All four family members (two affected siblings with epileptic encephalopathy and their parents) were analyzed. Clinical information, peripheral blood samples (individual II-1 and his parents), and the umbilical cord of individual II-2 were obtained after written informed consent was given. DNA was extracted using standard methods. Experimental protocols were approved by the institutional review board of Yokohama City University School of Medicine.

### Whole exome sequencing (WES)

Genomic DNA was captured using the SureSelect Human All Exon v4 Kit (51 Mb; Agilent Technologies, Santa Clara, CA, U.S.A.) and sequenced on an Illumina HiSeq2000 (Illumina, San Diego, CA, U.S.A.) with 101 bp paired-end reads. Exome data processing, variant calling, and variant annotation were performed as previously described.[9] *PIGO* mutations detected by WES were confirmed by Sanger sequencing, and searched for in the variant database of our 408 in-house control exomes. For individual II-2, only those *PIGO* mutations identified in individual II-1 were checked by Sanger sequencing.

### Flow cytometry

Surface expression of GPI-anchored proteins was examined as previously described.[8]

## Results

### Clinical features

A summary of the clinical features of individuals II-1 and II-2 is shown in Table S1. Both siblings had intractable seizures and severe developmental delay, which were compatible with epileptic encephalopathy.

### Case report 1

Individual II-1 is a 19-year-old male born to nonconsanguineous parents after a 38-week gestation with no asphyxia. His birth weight was 3,250 g (+0.5 standard deviation [SD]), height 52.0 cm (−1.4 SD), and head circumference 34.0 cm (−0.5 SD). Developmental milestones were delayed with no head control achieved at 6 months. At 1 year of age, he developed complex partial seizures with staring, crying, and irregular respiration leading to cyanosis. Brain magnetic resonance imaging (MRI) revealed no abnormalities (Fig. 1A,B). At 1 year and 11 months of age, he had intractable seizures refractory to valproate, zonisamide, and clonazepam. His body weight at this time was 10.54 kg (−0.8 SD), height 84.8 cm (−0.1 SD), and head circumference 45.3 cm (−1.9 SD). He was able to smile but unable to control his head or speak any meaningful words. He had a high arched palate and a tented mouth (Fig. 1E). His muscle tone was hypotonic, and deep tendon reflexes were normal with negative Babinski sign. Chorea was observed mainly in the upper extremities. He did not show brachytelephalangy or nail aplasia (Fig. 1F).

Interictal electroencephalography (EEG), motor conduction velocities, visual evoked potential, short-latency somatosensory evoked potentials, and electroretinogram were normal. Auditory brain responses revealed only wave I. Serum alkaline phosphatase (ALP) levels were 436 U/L (normal range, 145–420),[10] and calcium and phosphate levels were normal. Metabolic analysis including lactate, pyruvate, very long fatty acids, and organic acid showed no abnormalities. His epileptic attacks sometimes led to generalized tonic–clonic seizures. Ictal EEG showed rhythmic fast waves, which appeared at the left side of the central sulcus, followed by diffuse irregular spikes and waves. Phenytoin and bromide treatment slightly decreased the seizure frequency. He was often admitted to the hospital (>40 times) with respiratory insufficiency following upper respiratory tract infection and/or prolonged convulsions, and initiated home oxygen therapy at 2 years of age.

Swallowing and hand movement gradually deteriorated, and spastic quadriplegia and hypertonus with rigidity of both upper and lower limbs appeared at 4 years of age. At 6 years of age, his condition gradually deteriorated, and a brain MRI at 6 years of age revealed diffuse cerebral and cerebellar atrophy (Fig. 1C,D). ALP was slightly elevated at around 10 years of age (900 U/L [normal range 130–560]), followed by a gradual decrease at around the age of 19 (300 U/L [normal range 65–260]). At this time he required mechanical ventilation. He had a very severe intellectual disability and partial seizures with dyspnea every day, despite administration of phenytoin, valproic acid, phenobarbital, bromide, clobazam, and nitrazepam. Pyridoxine has not been administered.

### Case report 2

Individual II-2, the younger sister of individual II-1, was born without asphyxia. She did not show any facial dysmorphology or other congenital malformations. At 7 months of age, she developed generalized tonic–clonic seizures for which she was administered phenobarbital. At 1 year of age, she showed developmental delay with no head control. At this time, she was admitted to hospital due to epileptic convulsive status, and she died from multiorgan failure 3 days later. No autopsy was performed.

### Identification of *PIGO* mutations and flow cytometry analysis

We filtered out variants registered in dbSNP135 data and our in-house 91 control exomes, and narrowed down 193 rare protein-altering and splice-site variants (Table S2). Among them, we identified compound heterozygous mutations in two genes: *PIGO* (GenBank accession number

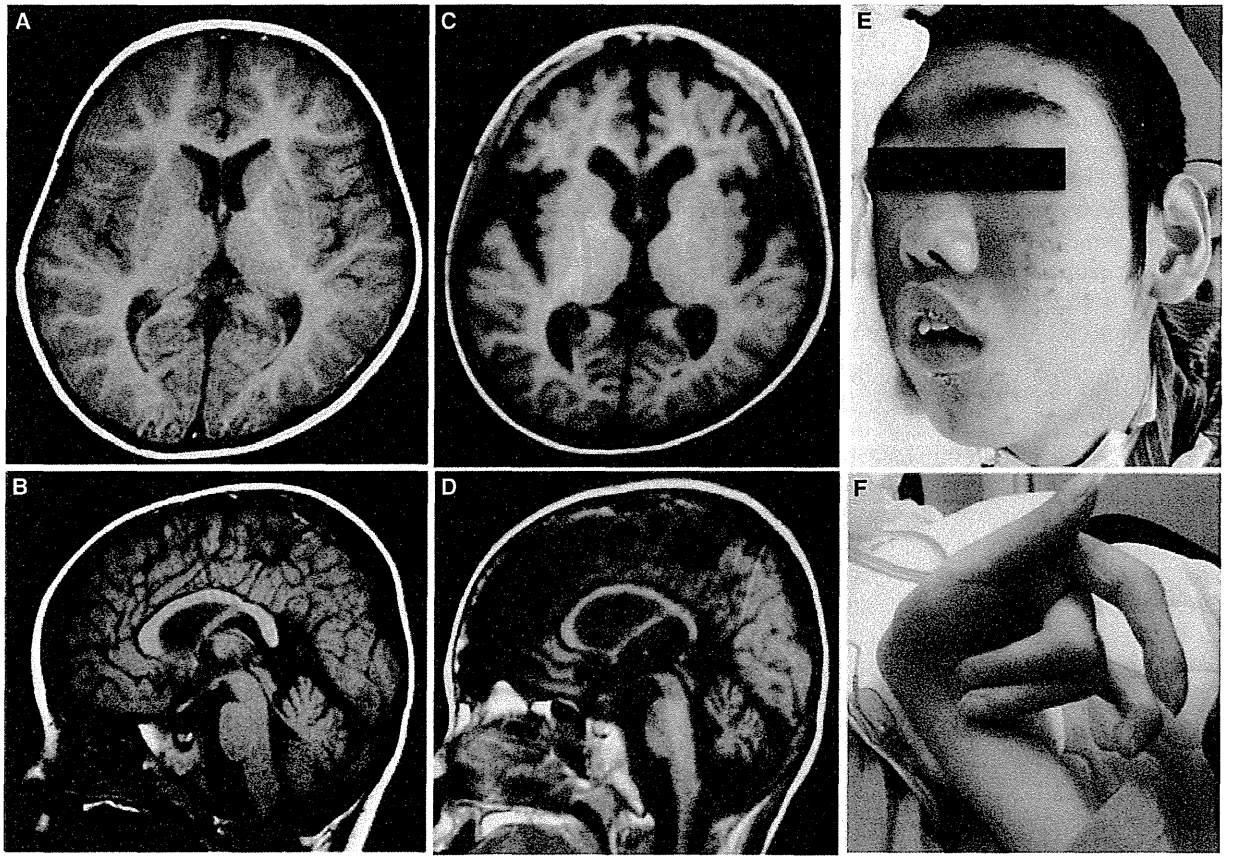


**Figure 1.**
$T_1$-weighted brain MRI of individual II-1. Axial (**A**) and sagittal (**B**) images revealed no signal or structural abnormalities at 1 year of age. Axial (**C**) and sagittal (**D**) images at 6 years of age showing diffuse cerebral and cerebellar atrophy. Facial (**E**) and hand (**F**) photographs of individual II-1 at 19 years of age showing tented mouth (**E**) and no anomalous fingers (**F**).


NM_032634.3) and *SCUBE1* (NM_173050.3) (Table S3). No homozygous mutation was detected. Four mutations are rare, but one of two mutations in *SCUBE1* is predicted as a polymorphism by web-prediction tools (Table S3). Therefore, *PIGO* mutations are the primary candidates. Two *PIGO* mutations were also found in his sister (individual II-2). A novel missense mutation c.389C>A (p.Thr130Asn) in exon 1 was inherited from their father and a novel nonsense mutation c.1288C>T (p.Gln430*) in exon 6 was inherited from their mother. Surface expressions of CD16 and CD24 on granulocytes from the individual II-1 were slightly, but clearly, decreased compared with a normal control and his mother, demonstrating GPI-anchor deficiencies in the patient (Fig. S1).

## Discussion

In this study, we report two siblings with severe epileptic seizures, developmental delay, and mild elevation of ALP caused by two novel compound heterozygous mutations in *PIGO*. In individuals II-1 and II-2 of the present study, the p.Thr130Asn mutation in *PIGO* is located in an alkaline phosphatase–like core domain, whereas the p.Gln430* mutation is expected to produce a truncated protein that lacks most transmembrane domains (Fig. 2B). To date, only three families with HPRMS are reported in association with compound heterozygous *PIGO* mutations: p.Leu957Phe and p.Thr788Hisfs*5 in the first family, p.Leu957Phe and c.3069+5G>A skipping exon 9 leading to c.2855_3069del (p.Val952Aspfs*24) in the second,[5] and c.355C>T (p.Arg119Trp) and c.2497_2498del (p.Ala834Cysfs*131) in the third.[8] These five mutations led to markedly decreased expression of CD16, CD24, and CD59 on granulocytes from the patient or failed to recover expression of GPI-anchored proteins in *PIGO*-deficient CHO cells, suggesting that expression of GPI-anchored proteins was severely impaired in the patients.[5,8] On the other hand, individual II-1 with p.Thr130Asn and p.Gln430* mutations showed mildly decreased expression of CD16 and CD24 on the surface of blood granulocytes. This difference in the expression of GPI-anchored proteins might be associated with lacking characteristic features of HPMRS in individual

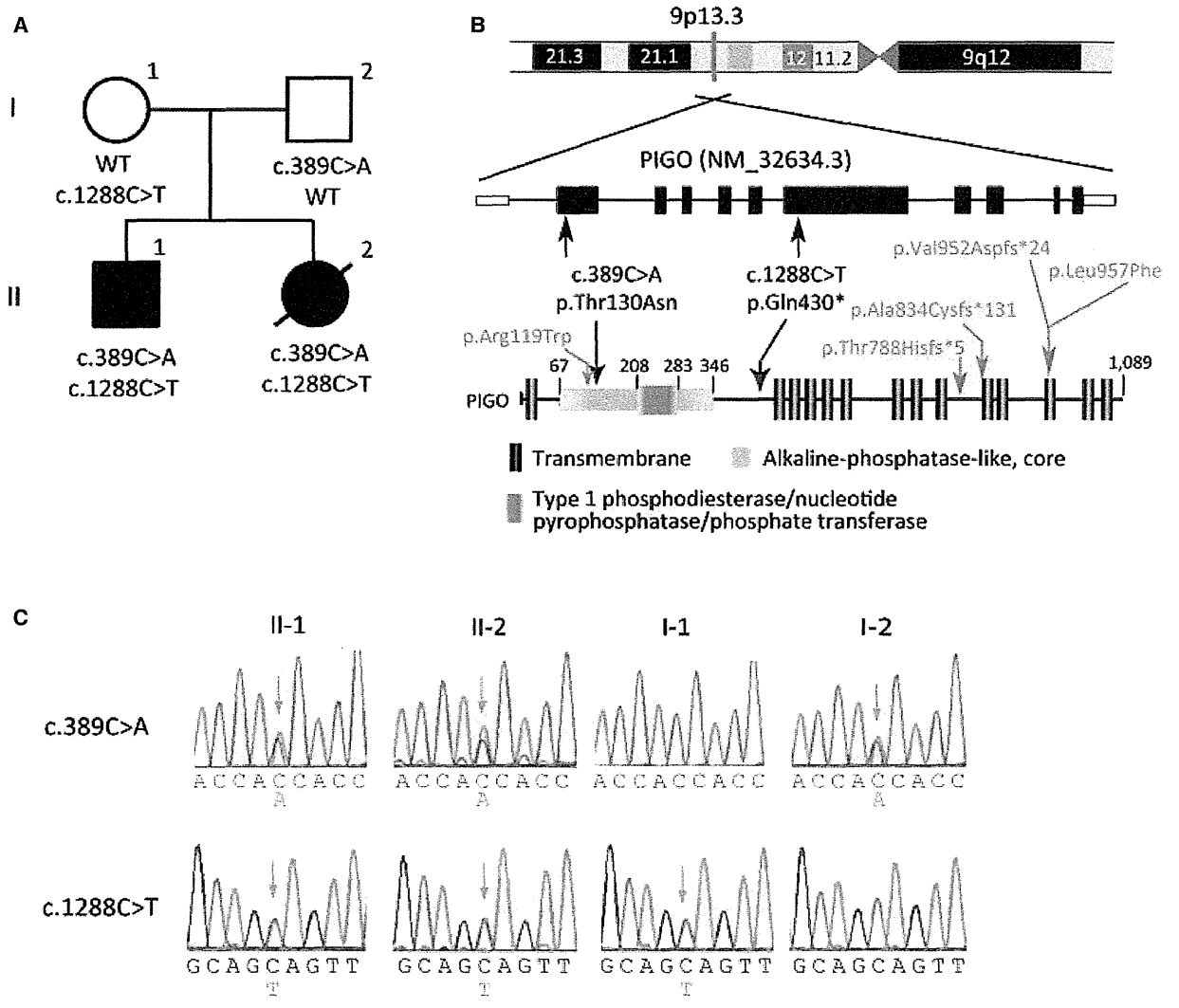


**Figure 2.**
(**A**) Familial pedigree of individuals I (II-1) and 2 (II-2). (**B**) Distribution of *PIGO* mutations. Previously reported mutations are highlighted in red. (**C**) Individuals II-1 and II-2 carrying compound heterozygous mutations in *PIGO*. Their mother (I-1) carried c.1288C>T (p.Gln430*), and their father (I-2) carried c.389C>A (p.Thr130Asn).
*Epilepsia* © ILAE

II-1, such as facial dysmorphic features, hypoplasia of distal phalanges, and elevation of serum ALP. Of interest, both patients in our report and a patient reported by Kuki et al. possessed missense mutations commonly in an alkaline phosphatase–like core domain, and showed progressive cerebral and cerebellar atrophy, and more severe intractable epilepsy and developmental delay than the other two families with *PIGO* mutations reported by Krawitz et al.[5,8] This fact raised a possibility that mutations in the alkaline phosphatase–like core domain can affect brain development and function more specifically regardless of expression of GPI-anchored proteins in blood granulocytes. Further accumulation of patients with *PIGO* mutations and functional analysis using neuronal cells are required for elucidating phenotype–genotype correlations in association with *PIGO* mutations.

Our data expand the clinical spectrum of GPI-anchor deficiencies to include epileptic encephalopathy. In addition, it has been recently reported that mutations in the *SLC35A2* encoding UDP-galactose transporter cause a congenital disorder of glycosylation in three patients, and five of them showed seizures with hypsarrhythmia pattern on electroencephalography.[11,12] Therefore, it is likely that abnormalities in glycosylation, including the GPI pathway, may be one of the underlying defects in epileptic encephalopathy.

In conclusion, we have described two siblings with epileptic encephalopathy that harbor novel compound

heterozygous mutations in *PIGO*. Further genetic analysis of GPI-anchor synthesis pathway is needed for the understanding of epileptic encephalopathy.

## Acknowledgments

We would like to thank the patients and their families for their participation in this study. We thank Aya Narita and Nobuko Watanabe for technical assistance. This work was supported by the Ministry of Health, Labour and Welfare of Japan; a Grant-in-Aid for Scientific Research (A), (B), and (C) from the Japan Society for the Promotion of Science (A: 24249019, B: 25293085 25293235, C: 23590363); the Takeda Science Foundation; the Japan Science and Technology Agency; the Strategic Research Program for Brain Sciences (11105137); and a Grant-in-Aid for Scientific Research on Innovative Areas (Transcription Cycle, Exploring molecular basis for brain diseases based on personal genomics) from the Ministry of Education, Culture, Sports, Science and Technology of Japan (12024421, 25129705).

## Disclosure

We confirm that we have read the Journal's position on issues involved in ethical publication and affirm that this report is consistent with those guidelines. None of the authors has any conflicts of interest to disclose.

## References

1. Kinoshita T, Fujita M, Maeda Y. Biosynthesis, remodelling and functions of mammalian GPI-anchored proteins: recent progress. *J Biochem* 2008;144:287–294.
2. Fujita M, Kinoshita T. GPI-anchor remodeling: potential functions of GPI-anchors in intracellular trafficking and membrane dynamics. *Biochim Biophys Acta* 2012;1821:1050–1058.
3. Freeze HH, Eklund EA, Ng BG, et al. Neurology of inherited glycosylation disorders. *Lancet Neurol* 2012;11:453–466.
4. Freeze HH. Understanding human glycosylation disorders: biochemistry leads the charge. *J Biol Chem* 2013;288:6936–6945.
5. Krawitz PM, Murakami Y, Hecht J, et al. Mutations in *PIGO*, a member of the GPI-anchor-synthesis pathway, cause hyperphosphatasia with mental retardation. *Am J Hum Genet* 2012;91:146–151.
6. Krawitz PM, Murakami Y, Riefl A, et al. *PGAP2* mutations, affecting the GPI-anchor-synthesis pathway, cause hyperphosphatasia with mental retardation syndrome. *Am J Hum Genet* 2013;92:584–589.
7. Hansen L, Tawamie H, Murakami Y, et al. Hypomorphic mutations in *PGAP2*, encoding a GPI-anchor-remodeling protein, cause autosomal-recessive intellectual disability. *Am J Hum Genet* 2013;92:575–583.
8. Kuki I, Takahashi Y, Okazaki S, et al. Vitamin B6-responsive epilepsy due to inherited GPI deficiency. *Neurology* 2013;81:1467–1469.
9. Saitsu H, Nishimura T, Muramatsu K, et al. *De novo* mutations in the autophagy gene *WDR45* cause static encephalopathy of childhood with neurodegeneration in adulthood. *Nat Genet* 2013;45:445–449.
10. Turan S, Topcu B, Gokce I, et al. Serum alkaline phosphatase levels in healthy children and evaluation of alkaline phosphatase z-scores in different types of rickets. *J Clin Res Pediatr Endocrinol* 2011;3:7–11.
11. Ng BG, Buckingham KJ, Raymond K, et al. Mosaicism of the UDP-galactose transporter *SLC35A2* causes a congenital disorder of glycosylation. *Am J Hum Genet* 2013;92:632–636.
12. Kodera H, Nakamura K, Osaka H, et al. *De novo* mutations in *SLC35A2* encoding a UDP-galactose transporter cause early-onset epileptic encephalopathy. *Hum Mutat* 2013;34:1708–1714.

## Supporting Information

Additional Supporting Information may be found in the online version of this article:

**Figure S1.** Expression of GPI-anchored proteins on granulocytes from the patient.

**Table S1.** Clinical features of individuals with *PIGO* mutations.

**Table S2.** Summary of the exome sequencing performance.

**Table S3.** Candidate variants corresponding to the autosomal recessive model.

CLINICAL REPORT

AMERICAN JOURNAL OF medical genetics

# Aortic Aneurysm and Craniosynostosis in a Family With Cantu Syndrome

**Yoko Hiraki,[1] Satoko Miyatake,[2] Michiko Hayashidani,[3] Yutaka Nishimura,[3] Hiroo Matsuura,[4] Masahiro Kamada,[5] Takuji Kawagoe,[6] Keiji Yunoki,[7] Nobuhiko Okamoto,[8] Hiroko Yofune,[9] Mitsuko Nakashima,[2] Yoshinori Tsurusaki,[2] Hirotomo Satisu,[2] Akira Murakami,[2] Noriko Miyake,[2] Gen Nishimura,[10] and Naomichi Matsumoto[2]***

[1]Hiroshima Municipal Center for Child Health and Development, Hiroshima, Japan

[2]Yokohama City University Graduate School of Medicine, Yokohama, Japan

[3]Medical Center for Premature and Neonatal Infants, Hiroshima City Hospital, Hiroshima, Japan

[4]Department of Pathology, Hiroshima City Hospital, Hiroshima, Japan

[5]Division of Pediatric Cardiology, Hiroshima City Hospital, Hiroshima, Japan

[6]Department of Cardiology, Hiroshima City Hospital, Hiroshima, Japan

[7]Department of Cardiovascular Surgery, Hiroshima City Hospital, Hiroshima, Japan

[8]Department of Medical Genetics, Osaka Medical Center and Research Institute for Maternal and Child Health, Osaka, Japan

[9]Hiroshima City Hokubu Center for Children's Treatment and Guidance, Hiroshima, Japan

[10]Department of Pediatric Imaging, Tokyo Metropolitan Children's Medical Center, Tokyo, Japan

Manuscript Received: 10 May 2013; Manuscript Accepted: 8 August 2013

Cantu syndrome is an autosomal dominant overgrowth syndrome associated with facial dysmorphism, congenital hypertrichosis, and cardiomegaly. Some affected individuals show bone undermodeling of variable severity. Recent investigations revealed that the disorder is caused by a mutation in *ABCC9*, encoding a regulatory SUR2 subunit of an ATP-sensitive potassium channel mainly expressed in cardiac and skeletal muscle as well as vascular smooth muscle. We report here on a Japanese family with this syndrome. An affected boy and his father had a novel missense mutation in *ABCC9*. Each patient had a coarse face and hypertrichosis. However, cardiomegaly was seen only in the boy, and macrosomia only in the father. Skeletal changes were not evident in either patient. Craniosynostosis in the boy and the development of aortic aneurysm in the father are previously undescribed associations with Cantu syndrome.



How to Cite this Article:
Hiraki Y, Miyatake S, Hayashidani M, Nishimura Y, Matsuura H, Kamada M, Kawagoe T, Yunoki K, Okamoto N, Yofune H, Nakashima M, Tsurusaki Y, Satisu H, Murakami A, Miyake N, Nishimura G, Matsumoto N. 2014. Aortic aneurysm and craniosynostosis in a family with Cantu syndrome.
Am J Med Genet Part A 164A:231–236.

**Key words:** Cantu syndrome; *ABCC9*; familial mutation; aortic aneurysm; craniosynostosis

Conflict of interest: none.

Grant sponsor: The Ministry of Health, Labour and Welfare of Japan; Grant sponsor: Japan Science and Technology Agency; Grant sponsor: Strategic Research Program for Brain Sciences; Grant sponsor: Ministry of Education, Culture, Sports, Science and Technology of Japan; Grant sponsor: Japan Society for the Promotion of Science; Grant sponsor: Takeda Science Foundation; Grant sponsor: Yokohama Foundation for the Advancement of Medical Science; Grant sponsor: Hayashi Memorial Foundation for Female Natural Scientists.

*Correspondence to:
Naomichi Matsumoto, Department of Human Genetics, Yokohama City University Graduate School of Medicine, 3-9 Fukuura, Kanazawa-ku, Yokohama 236-0004, Japan.
E-mail: naomat@yokohama-cu.ac.jp

Article first published online in Wiley Online Library (wileyonlinelibrary.com): 25 November 2013
DOI 10.1002/ajmg.a.36228

## INTRODUCTION

Cantu syndrome is an autosomal dominant malformation syndrome first described by Cantu in 1982. The hallmarks include prenatal overgrowth, congenital hypertrichosis, characteristic facial anomalies, and cardiomegaly [Cantu et al., 1982]. Some affected individuals show mild osteochondrodysplasia, that is, bone undermodeling of variable severity. Recent investigations have revealed the causal relationship between Cantu syndrome and mutations in *ABCC9* (ATP-binding cassette, subfamily c, member 9; OMIM 601439), alternatively termed *SUR2* (sulfonylurea receptor 2) [Harakalova et al., 2012; van Bon et al., 2012]. *ABCC9* mutations also have been found in dilated cardiomyopathy and familial atrial fibrillation. *ABCC9* encodes a K (ATP) channel (ATP-sensitive potassium channel) named ABCC9 that is mainly expressed in cardiac and skeletal muscle as well as vascular and nonvascular smooth muscle.

ABCC9 provides a unique feedback between cell metabolism and electrical activity. It plays an important role in protection for ischemic stress in the heart, protection against fiber damage in skeletal muscle, and control of vasomotor tone in smooth muscle, when cellular energetics are endangered [Flagg et al., 2010]. This protective role accounts for the cardiac phenotype in Cantu syndrome as well as the pathogenic relation between *ABCC9* and genetic heart diseases. Moreover, as ABCC9 has affinity for sulfonylurea, it is presumed to act as a sulfonylurea receptor. That may be the reason why it can regulate paracellular permeability in gastrointestinal, renal and liver tissues [Jons et al., 2006].

Here, we report on a family with Cantu syndrome. An affected boy and his father had a novel *ABCC9* mutation. The unique manifestations in this family were craniosynostosis in the boy and thoracic aortic aneurysm in the father.

## CLINICAL REPORT

### Patient 1

The 4-year-old boy was the first child born to unrelated parents (a 29-year-old mother and 27-year-old father). His father was similarly affected.

The pregnancy had been complicated by transient oligohydramnios only during the second trimester. Prenatal ultrasound during the third trimester continuously demonstrated pericardial effusion. Patient 1 was born by cesarean section at 37 weeks of gestation. Birth weight was 2,000 g (−1.95 SD), length 46.5 cm (−0.5 SD), and OFC 32.5 cm (−0.1 SD). Hypertrichosis, macroglossia, and umbilical hernia with excessive skin were noted at birth. The neonatal course was complicated by hyperbilirubinemia, hypocalcemia, and thrombocytopenia. Fifty days after birth he developed respiratory distress unassociated with any respiratory infectious signs, which required respiratory support that was continued for 2 months. Imaging showed cardiomegaly (CTR 0.54), increasing pericardial effusion, left ventricular dilatation (LVDd: 143% of the normal), and pulmonary hypertension with patency of the foramen of ovale. NT-proBNP was 13,189 pg/ml (standard range: up to 125 pg/ml). Two months later, pulmonary hypertension ameliorated, but left ventricular (LV) dilatation persisted and cardiomegaly increased. At age 8 months, echocardiography showed normal cardiac function and LVDd, and only a small amount of pericardial effusion. NT-proBNP decreased (136 pg/ml). He had febrile convulsion twice at ages $1^{3}/_{12}$ and $2^{11}/_{12}$ years, but electroencephalography yielded a normal result. He underwent surgical treatment for umbilical hernia at age $2^{8}/_{12}$ years. He had hematochezia with unknown etiology even after anosigmoidoscopy at age $2^{8}/_{12}$ years.

At age $2^{9}/_{12}$ years, he was referred to us for evaluation of multiple anomalies. Physical findings included generalized hypertrichosis, muscular build, hyperpigmentation, soft "doughy" skin with deep palmar/planter crease, and characteristic facial appearance, including long face, full cheeks, thick eyebrows, puffy eyelids, epicanthus folds, depressed nasal bridge, anteverted nostrils, long philtrum, and large mouth with thick vermilion to the lips (Fig. 1A). The hands and feet were broad with clinodactyly of the 5th fingers. Height was 89.3 cm (−0.6 SD), weight 12.6 kg (−0.4 SD), and OFC 47 cm (−1.4 SD). Echocardiography demonstrated normal cardiac function (LV ejection fraction; 64%) and a trace amount of pericardial effusion. Skeletal survey showed only minimum broadening of ribs (Fig. 1B). Skull radiographs and 3D-CT displayed premature fusion of the sagittal and coronal sutures (Fig. 1C–E). Brain MRI indicated copper beaten findings of calvaria and normal brain structures (Fig. 1F). He was diagnosed as having mild psychomotor delay (DQ 55 at $3^{6}/_{12}$ years) and an autistic disorder based on the DSM-IV.

### Patient 2

The father of the proband was vaginally delivered at 42 weeks of gestation. Macrosomia (birth weight; 4,500 g +3.3 SD) and congenital hypertrichosis were noted at birth. He was reported to have recurrent upper respiratory tract infection in infancy. His medical history included repeated reports of abnormal electrocardiograms indicating incomplete right bundle branch block at health check in school and at his place of work. He sometimes felt palpitations that persisted for a while. He experienced several cryptogenic episodes of hematochezia, but no particular examination was performed. He was an enthusiastic basketball-player during high school. His paternal grandfather had been treated with a cardiac pacemaker. His maternal uncle was affected with dilated cardiomyopathy.

We evaluated him when he was 30 years old. Height was 173.0 cm (+0.4 SD), weight 69.0 kg (+1.3 SD), and OFC 60.5 cm (+2.1 SD). He had general hypertrichosis, soft skin, and a "coarse" facial appearance, including long face, puffy eyelids, long palpebral fissures, broad nose with flared nares and high nasal bridge, and thick vermilion to the lips. Radiological examinations revealed thoracic aortic aneurysm (Fig. 2A,B). Holter electrocardiogram yielded a normal result. Echocardiography showed almost normal cardiac function (LV ejection fraction; 65%), other than minimum tricuspid regurgitation. There were no signs of cardiac enlargement. Skeletal survey and laboratory examinations were unremarkable. At age 31 years, he underwent surgical intervention for thoracic aneurysm.

On histologic examination of the aneurysm, the tunica media showed diffuse mucopolysaccharide accumulation between the smooth muscle cells, enlarging the tissue gaps and forming cysts (cystic medial degeneration). The inner media was hypertrophic with nodular protrusions caused by irregular and reticulated

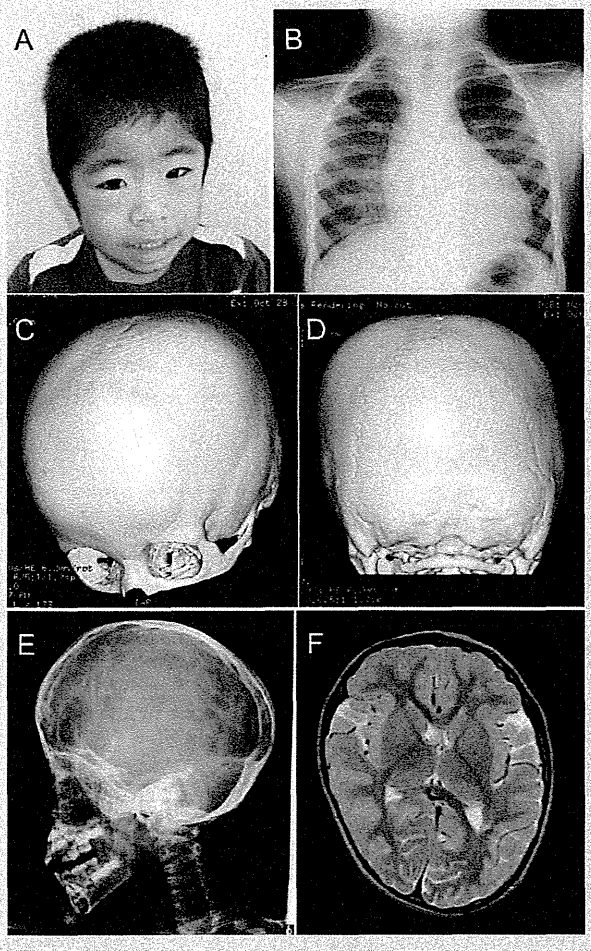


FIG. 1. Photograph of patient 1 at $2^{3}/_{12}$ years of age. A: "Coarse" facial appearance including long face, full cheeks, thick eyebrows, puffy eyelids, epicanthus folds, depressed nasal bridge with anteverted nostrils, long philtrum, and large mouth with thick vermilion to the lips. B: Chest radiograph showing cardiomegaly (CTR 0.65). C,D: Skull 3D-CT showing synostosis of bilateral coronal sutures and anterior aspect of the sagittal suture. E: Skull radiograph showing impression of cerebral gyri. F: Brain MRI showing scalloping of the calvarial inner table and normal brain structures.

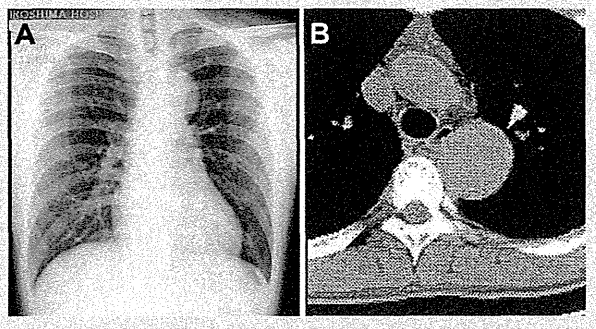


FIG. 2. Imaging studies of Patient 2 at 30 years. A: Chest radiograph showing the projection of aortic arch. B: Chest 3D-CT demonstrating fusiform dilation of the descending thoracic aorta.

hyperplasia of the smooth muscle cells. Excess mucoid deposition and hyperplasia of the collagen fibers between the smooth muscle cells resulted in fragmentation, reduction, and separation of elastic fibers (Fig. 3).

## CYTOGENETIC AND MOLECULAR ANALYSIS

In both patients, G-banded chromosomal analysis (550 band resolution) of blood lymphocytes yielded normal results. Copy number analysis on the proband using an Affymetrics Cytoscan HD array (Affymetrix, Santa Clara, CA) revealed two deletions which were inherited from his affected father: a 46 kb-deletion at 3q29, and a 49 kb-deletion at 1q31.3. However neither of the deleted regions contained any strong candidates for a causative gene. With the parent's informed consent, whole exome sequencing was performed on the proband (Patient 1), his affected father (Patient 2) and his unaffected mother. Genomic DNA (3 μg) was captured using a SureSelect$^{XT}$ Human All Exon 50 Mb Kit (Agilent Technologies, Santa Clara, CA) and sequenced on an Illumina HiSeq2000 with 108 bp pair-end reads. Image analyses and base calling were performed by sequence control software real time analysis and CASAVA software v1.8 (Illumina, San Diego, CA). Reads were aligned to GRCh37 with Novoalign (Novocraft Technologies, Selangor, Malaysia), and duplicate reads were marked using Picard (http://picard.sourceforge.net/) and excluded from downstream analysis. Local realignments around indels and base quality score recalibration were performed by the Genome Analysis Toolkit (GATK) [DePristo et al., 2011]. Single-nucleotide variants and small indels were identified using the GATK UnifiedGenotyper, and filtered according to the Broad Institute's best-practice guidelines v3. Variants registered in dbSNP135 (http://www.ncbi.nlm.nih.gov/projects/SNP/), which were not flagged as clinically associated, were filtered. Filter passed variants were annotated using ANNOVAR [Wang et al., 2010].

Mean coverage depth was 125-fold. To identify the pathogenic mutation, we excluded synonymous variants, or variants found in 132 in-house control exomes from the 2,634 filter-passed variants, and included only variants which were shared by proband and his affected father. Among 173 such variants, we identified a heterozygous novel missense mutation (c.3605C > T, p.T1202M) in the *ABCC9* gene that was carried by both patients (Fig. 4). The T1202 residue is evolutionarily conserved. Two out of three web-based prediction programs predicted this mutation to have a deleterious effect on protein function (SIFT; tolerated, PolyPhen2; probably damaging, MutationTaster; disease causing). The mutation has not been identified in any of 5,400 publicly available exomes (Exome Variant Server, National Heart, Lung, and Blood Institute (NHLBI) Exome Sequencing Project, http://evs.gs.washington.edu/EVS/).